Sensors & Diagnostics

TUTORIAL REVIEW

View Article Online
View Journal | View Issue

Cite this: *Sens. Diagn.*, 2025, **4**, 1060

Advancements in smart electrochemical gas sensors: bridging IoT, self-powering, and machine learning for healthcare

Hongyang Guo,[a] Zhuoru Huang,[a] Xiaojing Zhang,[a] Haoting Zhang,[a] Jiaying Sun,[a] Yuzi Zeng,[a] Yanjie Hu,[b] Yong Zhou,[b] Hao Wan*[ac] and Ping Wang *[ac]

Received 28th May 2025,
Accepted 3rd September 2025

DOI: 10.1039/d5sd00077g

rsc.li/sensors

Electrochemical gas sensors have attracted significant attention due to their high sensitivity and selectivity in detecting various gases. Recent advancements in microelectronics, materials science and computational technologies have driven the development of smart electrochemical gas sensors, enhancing their functionality with improved miniaturization, real-time data analysis, and remote monitoring capabilities. Furthermore, the integration of the internet of things, self-powered technologies and machine learning has expanded the potential of these sensors, enabling smart healthcare systems to adapt to complex and dynamic environments just as humans do. This paper reviews the basic sensing mechanisms, detection methods, recent developments of three types of electrochemical gas sensors and the related fabrication techniques. In addition, we further review their applications in three fields including air monitoring, breath analysis and microfluidic integration. Finally, current challenges, limitations, and future prospects are addressed, emphasizing the need for improved stability, selectivity, and energy efficiency to develop the next generation of electrochemical gas sensors.

1. Introduction

Human health is strongly affected by the quality of inhaled air. Exposure to hazardous gases and air pollutants—such as carbon monoxide (CO), nitrogen oxides (NO), sulfur dioxide, and particulate matter—can directly damage the respiratory and cardiovascular systems, and long-term exposure has been associated with chronic respiratory diseases, cancer, and neurological disorders.[1] These risks emphasize the necessity of precise and continuous monitoring of toxic gases in the environment to safeguard public health.

Beyond exogenous contaminants, endogenous volatile organic compounds (VOCs) generated by human metabolism have emerged as promising non-invasive biomarkers for disease diagnosis. More than 2000 VOCs have been identified in exhaled breath, spanning aldehydes, ketones, alcohols, hydrocarbons, and nitrogen- or sulfur-containing species.[2] Their concentrations and profiles vary significantly with pathological conditions. For instance, elevated fractional exhaled nitric oxide (FeNO) is a clinically validated marker of eosinophilic airway inflammation in asthma and chronic obstructive pulmonary disease (COPD), while CO has been used as an indicator of smoking exposure and oxidative stress. In the context of cancer, oxidative stress–derived aldehydes and hydrocarbons have been consistently reported as potential markers of lipid peroxidation processes. Ketones such as acetone have been associated with altered glucose metabolism and may reflect systemic metabolic disorders. Moreover, microbial infections give rise to characteristic volatilomes, including sulfur-containing compounds, alcohols, and ketones, which can serve as discriminatory infection biomarkers.[3] Collectively, these disease-specific alterations in breath VOC profiles highlight the promise of respiratory detection for non-invasive disease detection, clinical monitoring, and personalized healthcare strategies.

Gas sensors mimic the human olfactory system and provide a practical means to detect both environmental gases and disease-related VOCs, thereby linking environmental exposure and clinical diagnostics. While conventional analytical tools such as gas chromatography-mass spectrometry offer excellent sensitivity and selectivity, they are constrained by high cost, bulky instrumentation, and operational complexity.[4] Optical gas sensors are also suitable for trace gas detection but are limited by environmental interferences and technological complexity.[5,6] In contrast, emerging gas sensor technologies combine portability, low power consumption, and real-time detection, making them highly suitable for healthcare applications. In particular,

[a] *Biosensor National Special Laboratory, Key Laboratory of Biomedical Engineering of Education Ministry, Department of Biomedical Engineering, Zhejiang University, Hangzhou, 310027, China. E-mail: wh1816@zju.edu.cn, cnpwang@zju.edu.cn*
[b] *Department of Respiratory Medicine, Sir Run Run Shaw Hospital, School of Medicine, Zhejiang University, Hangzhou, 310016, China*
[c] *Binjiang Institute of Zhejiang University, Hangzhou, 310053, China*

electrochemical sensors are highly attractive for integration into compact and wearable platforms, as they enable continuous monitoring of breath biomarkers through their low power demand, miniaturized form factor, and direct conversion of redox reactions into electrical signals.[7] The development of high-performance gas sensors optimized for medical use therefore represents a critical step toward advancing early disease screening, precision diagnostics, and long-term health management.

In recent years, the concept of smart gas sensors has attracted growing attention, particularly in response to the increasing demand for precise, real-time, and personalized healthcare monitoring.[8–10] Smart gas sensors integrate multiple technologies—such as the internet of things (IoT), self-powered technologies, and machine learning (ML)—to achieve advanced functionality. These technologies mirror certain biological processes: IoT reflects the way neural tissues transmit sensory signals to the brain, self-powered technologies resemble the body's ability to generate and sustain energy, and ML mimics the brain's capacity for cognition and decision-making. Through such integration, smart gas sensors move beyond simple detection to intelligent systems capable of processing, interpreting, and responding to complex gas information (Fig. 1). The rapid advancement of these technologies is driving a paradigm shift in gas sensing from traditional hardware-based devices to multifunctional intelligent platforms. Importantly, smart gas sensors have already shown promising results in

Hongyang Guo received his B.E. degree of Electronic Science and Technology from Nanjing University of Information Science & Technology in 2024. Now he is a master student of biomedical engineering of Zhejiang University. His current research interests are focused on electrochemical gas sensors and the development of intelligent systems.

Zhuoru Huang received her bachelor's degree in biomedical engineering from Zhejiang University, PR China in 2021. Now she is a Ph.D. student of biomedical engineering at Zhejiang University. Her work includes the research of chemical sensors and electrochemical gas sensors.

Xiaojing Zhang received her B.E. degree of biomedical engineering in Zhejiang University, PR China in 2021. Now she is a Ph.D. student of biomedical engineering of Zhejiang University, PR China. Her research interests include surface acoustic wave sensors and biosensor instrument establishing for disease biomarker detection.

Haoting Zhang received his B.S. degree in Intelligent Science and Technology from Northeast Electric Power University in 2019 and his M.S. degree in Electronic Information from Northeastern University in Shenyang, China, in 2023. He is currently pursuing his Ph.D. degree at the College of Biomedical Engineering and Instrument Science, Zhejiang University. His current research interests are focused on flexible/stretchable electronic devices, as well as self-driven sensors and systems.

Jiaying Sun received her B.E. degree of biomedical engineering in Zhejiang University, PR China in 2022. Now she is a master student of biomedical engineering of Zhejiang University, PR China. Her research interests are gas sensors and the detection of disease markers in human exhaled gas.

Yuzi Zeng is now an undergraduate student at Zhejiang University, working on electrochemical gas sensors.

Yanjie Hu received her B.S. degree in internal medicine and Ph.D. degree in respiratory medicine from Zhejiang University, PR china in 2006, 2010, respectively. She is now the associate chief physician at the Run Run Shaw Hospital School of Medicine, Zhejiang University School of Medicine.

Yong Zhou received his B.S. degree in clinical medicine and Ph.D. degree in respiratory medicine from Zhejiang University, PR china in 2001, 2007, respectively. Now he the chief physician of clinical medicine at Run Run Shaw Hospital, Zhejiang University School of Medicine.

Hao Wan received his B.S. and Ph.D. degree in Biomedical Engineering from Huazhong University of Science and Technology, Wuhan, China and Zhejiang University, Hangzhou, China in 2010 and 2015, respectively. From 2015 to 2017, he worked as a postdoc in Electrical and Computer Engineering, Michigan State University, USA. Starting from 2017, he worked in the Department of Biomedical Engineering, Zhejiang University, China. His research interests are sensor microfabrication, electrochemical sensing and instrument development in environmental monitoring applications.

Ping Wang received his B.E. degree, M.S. degree and Ph.D. degree of electrical engineering in Harbin Institute of Technology, PR china in1984, 1987, and 1992, respectively. Now he is a professor of Biosensors National Special Lab, Department of Biomedical Engineering of Zhejiang University, PR China. His research interests include biomedical sensors, chemical sensors and measurement.

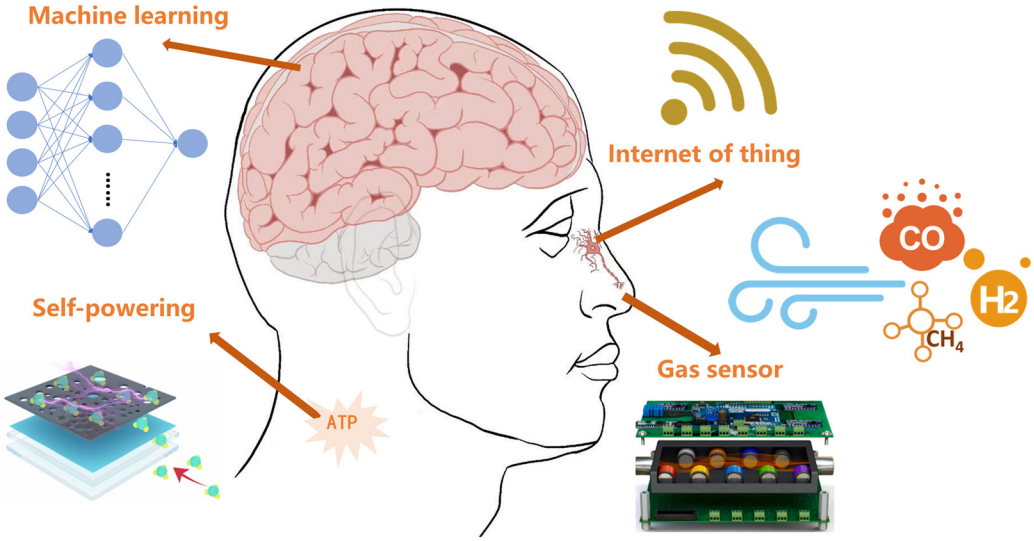

Fig. 1 A human-like smart system.

healthcare applications, such as monitoring exhaled breath biomarkers and tracking physical signs in real time.[11–13] Beyond healthcare, they are also being explored in air pollution monitoring,[14–16] mine safety,[17–19] drug control,[20–22] and food safety.[23–25] This integration of sensing, communication, and intelligence therefore represents a key step toward establishing gas sensors as indispensable tools for next-generation healthcare and environmental protection.

By integrating chemistry, electronics, and advanced materials, electrochemical gas sensors can demonstrate high-precision detection capabilities across a broad spectrum of applications,[26] which means that combining electrochemical gas sensors with smart technologies can show strong development potential. In recent years, several reviews have been published on the topic of electrochemical sensors for gas detection and smart sensor systems. Zhang *et al.*[27] introduced an enzyme-based electrochemical gas sensor, demonstrating how biomolecular recognition can be coupled with electrochemical transduction to achieve high selectivity in gas detection. From a system-level perspective, Zong *et al.*[10] emphasized the development and application of smart gas sensors, focusing on how IoT integration, artificial intelligence algorithms, and multifunctional system designs are reshaping gas sensing into intelligent platforms capable of real-time analysis and decision-making. In parallel, Atkare *et al.*[28] provided a perspective on 2D MXene-based materials for self-powered smart gas sensors, underscoring their potential for autonomous operation and stable performance without external energy input. Complementarily, Cao *et al.*[29] reviewed triboelectric nanogenerator (TENG)-based human–machine interaction systems, exploring how the integration of TENGs with IoT architectures offers a sustainable route toward energy-autonomous sensing and interactive healthcare technologies. Finally, Banga *et al.*[30] critically assessed advances in gas detection methodologies, including electrochemical and spectroscopic techniques, with a special focus on environmental and health-related monitoring, thus setting a broad context for the healthcare-oriented discussion of electrochemical gas sensors. While the above reviews have provided valuable insights into electrochemical gas sensors and smart sensing technologies, most remain limited in scope. They tend to emphasize specific aspects—such as individual sensing materials, isolated transduction mechanisms, or the prospects of a single technology—without offering a holistic view that integrates these dimensions. Consequently, although these works enrich our understanding of materials design, system integration, and intelligent functionalities, they do not provide a comprehensive overview of smart electrochemical gas sensors from the perspective of healthcare applications. Furthermore, even when applications are mentioned, the focus has largely been on domains such as environmental monitoring, food safety, or industrial detection, with only marginal attention paid to healthcare-related contexts. What is still missing is a multidimensional analysis that connects sensing principles, material strategies, system-level intelligence, and microfluidic integration, all framed explicitly around the needs of human health monitoring and disease diagnostics. In this review, we aim to fill this gap by systematically summarizing the working principles, signal transduction pathways, detection methods and related Fabrication techniques of smart electrochemical gas sensors, with a particular emphasis on their recent breakthroughs in healthcare-related scenarios. We further highlight strategies for enhancing selectivity, accuracy, and sensitivity through the integration of IoT, self-powered technologies, and ML algorithms. Special attention is given to emerging concepts such as remote and on-site gas sensing, where wireless communication and artificial intelligence enable air quality assessment, real-time breath monitoring and microchannel control (Fig. 2). Finally, we discuss the major challenges and limitations that remain in this field, as well as potential future directions that may drive

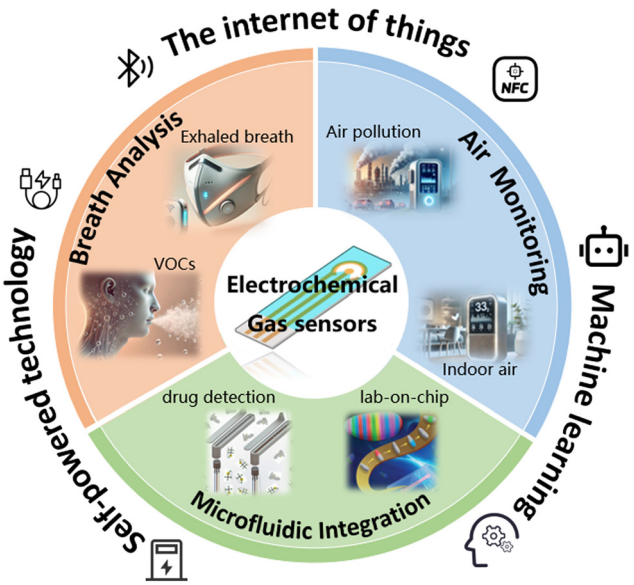

Fig. 2 Applications of smart electrochemistry gas sensor in healthcare.

the development of next-generation smart electrochemical gas sensors for healthcare.

2. Sensing mechanism of electrochemical gas sensors

2.1 Basic principle

Electrochemical gas sensors operate by exploiting redox reactions at the electrode–electrolyte interface, where target gas molecules undergo oxidation or reduction, and the resulting charge transfer is transduced into electrical signals such as current, potential, or impedance. Owing to the direct chemical interaction with analytes, these sensors inherently exhibit high sensitivity and selectivity compared with many other gas sensing mechanisms. In contrast, metal oxide semiconductor (MOS) sensors detect gases through changes in surface conductivity caused by gas adsorption and desorption processes, which typically require elevated operating temperatures (200–400 °C) to activate, leading to higher power consumption and reduced stability.[31] Optical sensors, including utilizing light-induced acoustic/elastic techniques, measure gases *via* light–matter interactions and offer excellent accuracy and fast response. However, their susceptibility to environmental conditions limit their wide application.[32] Gas chromatography-mass spectrometry (GC-MS) achieves outstanding sensitivity and selectivity, yet its size, cost, and need for specialized operation prevent real-time or point-of-care deployment.[33] These comparisons highlight that electrochemical gas sensors uniquely combine miniaturization, low energy demand, and direct signal transduction, making them particularly advantageous for healthcare-related applications.

Electrochemical sensors typically consist of an electrolyte and a three-electrode system. Electrolytes are categorized as liquid electrolyte,[34,35] gel electrolyte[36,37] and solid electrolytes[38,39] according to their physical state. The electrolyte not only provides an ion-conducting pathway but also significantly influences sensitivity, detection limit, and stability. For example, Singh *et al.*[35] demonstrated that electrolyte engineering directly governs performance: adding diols (ethylene glycol, 1,2- and 1,3-propanediol) to the RTIL $[C_2mim][NTf_2]$ increased NH_3 solubility and reduced viscosity, thereby enhancing amperometric sensing. Dong *et al.*[40] built an all-solid-state electrochemical sensing platform using a $Na_4Zr_2Si_3O_{12}$ (NZS) solid electrolyte and solid-state reference electrode; the device, prepared by high-temperature solid-state synthesis (400 °C, 40 MPa), showed robust operation in aqueous and simulated seawater with strong linearity ($R^2 > 0.99$), broad detection ranges, and low detection thresholds for pH. Zhong *et al.*[41] systematically compared gel electrolytes—hydrogels, eutectogels, and iongels—for OECTs and showed that a eutectogel (poly(glycerol-1,3-diglycerolate diacrylate) + choline chloride/1,3-propanediol DES) delivered the best transient and steady-state performance and superior durability, giving higher ECG signal amplitudes and SNR under continuous operation (5 h) and in daily measurements over 30 days. Moreover, a typical three-electrode system, including a working electrode (WE), an opposing electrode (CE) and a reference electrode (RE). The WE is where the target reaction occurs and is commonly composed of materials such as glassy carbon or metal electrodes. The CE is responsible for completing the electrical circuit and is typically made from inert materials, such as platinum or graphite, to ensure it does not directly affect the measurement outcome. The RE provides a stable and known reference potential, allowing for precise determination of the WE potential, with common types including the saturated calomel electrode and the silver/silver chloride (Ag/AgCl) electrode.[42] During electrochemical gas detection, the target gas diffuses to the surface of the WE, where oxidation or reduction reactions take place, leading to changes in the electrical signal. Electrochemical gas sensors often employ various sensing elements, including noble metal nanomaterials (such as platinum and gold),[43,44] conductive polymers (such as polyaniline and polypyrrole),[44,45] MOS nanomaterials (such as ZnO and SnO_2),[46,47] and carbon-based materials (such as graphene oxide (GO) and carbon nanotubes (CNT)).[48,49] These sensing elements typically exhibit advantages such as high specific surface area, excellent catalytic activity, and good electrical conductivity, facilitating gas molecule adsorption and reaction on the WE surface, thereby enhancing the sensor's response and recovery speed.[50,51] Moreover, the sensing electrode consists mainly of sensitive and three-electrode system including transduction elements. The sensitive element directly contacts and reacts with the target substance, providing selective recognition and response capability for the substance under test. The role of the transduction element is to convert the non-electrical information generated by the sensitive element into an electrical signal that is easy to

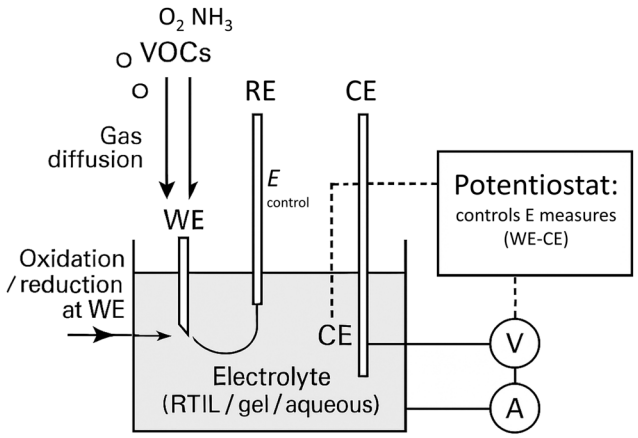

Fig. 3 Schematic illustration of the three-electrode system of the electrochemical gas sensor.

measure and process. By designing different sensitive elements, the selectivity of different substances can be improved, and the study of different conversion elements helps to overcome the application obstacles of sensors. Fig. 3 is a schematic illustration of an electrochemical gas sensor with a three-electrode configuration (WE, CE, RE). Gas molecules diffuse to the working electrode, where redox reactions occur. The resulting electrochemical signal is transmitted through the electrolyte and recorded as a measurable current or potential.

2.2 Electrochemical detection methods

Various electrochemical sensors employ different detection techniques, with cyclic voltammetry (CV), chronoamperometry (CA), and electrochemical impedance spectroscopy (EIS) being the most commonly used methods. Depending on the type of converted signal, electrochemical sensors can be classified into amperometric, potentiometric, and impedimetric types.

CV applies a triangular waveform linear potential scan signal to the electrode surface while recording the current response during the potential sweep. When the potential reaches the oxidation or reduction potential of the target gas, a corresponding electrochemical reaction occurs, generating oxidation and reduction peaks.[52] By analyzing parameters such as peak current magnitude and peak potential position, qualitative and quantitative analysis of the target gas can be performed. Since different gases undergo redox reactions at distinct potentials on the electrode surface, oxidation and reduction peaks characteristic of each gas appear in the cyclic voltammogram when gas molecules react on the WE. The peak positions can be used for the qualitative identification of gas species. Additionally, under specific conditions, the oxidation or reduction peak current in the cyclic voltammogram shows a proportional relationship with the gas concentration, enabling the quantitative determination of gas concentration from the peak current. CV is frequently employed for screening and optimizing sensor-sensitive materials, facilitating the evaluation of material modification effectiveness. When developing new gas sensors, CV is used to examine the response characteristics of various sensing materials to the target gas, guiding the selection of the optimal sensing material.

CA is classified as a constant voltage technique, where a fixed potential is applied to the electrode, and the current response is monitored over time.[52] In a chronoamperometric experiment, applying a potential step to the electrode triggers an electrochemical reaction at the electrode surface, leading to changes in the reactant concentration near the electrode and establishing a concentration gradient that drives mass diffusion. Under diffusion control, the measured current can serve as a quantitative indicator of the target gas concentration, following the Cottrell equation: $i = \frac{nFAc_j^0\sqrt{D}}{\sqrt{\pi t}}$, where i is the current (A), n is the number of electrons transferred in the electrode reaction, F is the Faraday constant, A is the electrode area (cm^2), D is the diffusion coefficient of the reactant, c_j^0 is the bulk concentration of the reactant (mol cm^{-3}), and t is time (s). CA is particularly well-suited for real-time and continuous monitoring due to its fast response, straightforward data processing, and high sensitivity, allowing the detection of subtle current variations and facilitating the effective measurement of low-concentration gases.

EIS involves applying a small-amplitude sinusoidal voltage (or current) and measuring the response signal of the electrode system, which follows an approximately linear relationship. This method provides impedance information while minimizing disturbances to the studied surface.[53] After obtaining the impedance data, impedance spectrum analysis is performed. Common impedance spectra include the Bode plot and the Nyquist plot. By analyzing these spectra, key electrical parameters of the sensor, such as resistance, capacitance, and inductance, can be determined, along with critical information regarding electrode reaction kinetics and diffusion processes. This analysis serves as a valuable basis for a deeper understanding of the reaction mechanisms and performance of electrochemical systems.

2.3 Electrochemical gas sensors

Amperometric electrochemical sensors represent the most prevalent type of gas electrochemical sensors. Their operating principle involves the diffusion of the target gas onto the WE surface, where a redox reaction occurs, generating a current that quantitatively correlates with the concentration of the target analyte. CV and CA are the primary electrochemical detection techniques used in amperometric gas sensors. Zhi *et al.* developed an amperometric hydrogen sensor utilizing a Pt/C/Nafion screen-printed carbon electrode (SPCE) combined with a solid polymer electrolyte.[54] CV and CA were used to measure hydrogen concentration, with the electrode structure and detection results illustrated in (Fig. 4a). The sensor demonstrated a sensitivity of 0.1 nA

ppm^{-1}, a limit of detection (LOD) of 6.3 ppm, and excellent linearity. Klun *et al.* proposed a gaseous hydrogen peroxide (H_2O_2) amperometric sensor based on a copper redox mediator, utilizing an aqueous polyacrylate gel electrolyte containing Cu(II) to enable rapid and sensitive detection of gaseous H_2O_2.[55] This sensor features a wide linear range (10–100 mg m^{-3}), a low LOD (0.53 mg m^{-3}), and a fast response time within 2 minutes (Fig. 4b). Zuo *et al.*[56] introduced an amperometric sensor incorporating one-dimensional (1D) platinum nanotubes (Pt NTs) for ultra-sensitive hydrogen sulfide (H_2S) detection. The sensor demonstrated outstanding performance, achieving an LOD as low as 0.025 ppb, with response and recovery times under 1 second. It also offers a wide detection range (100–0.025 ppb), high selectivity, strong repeatability, and excellent long-term stability, presenting a new strategy for

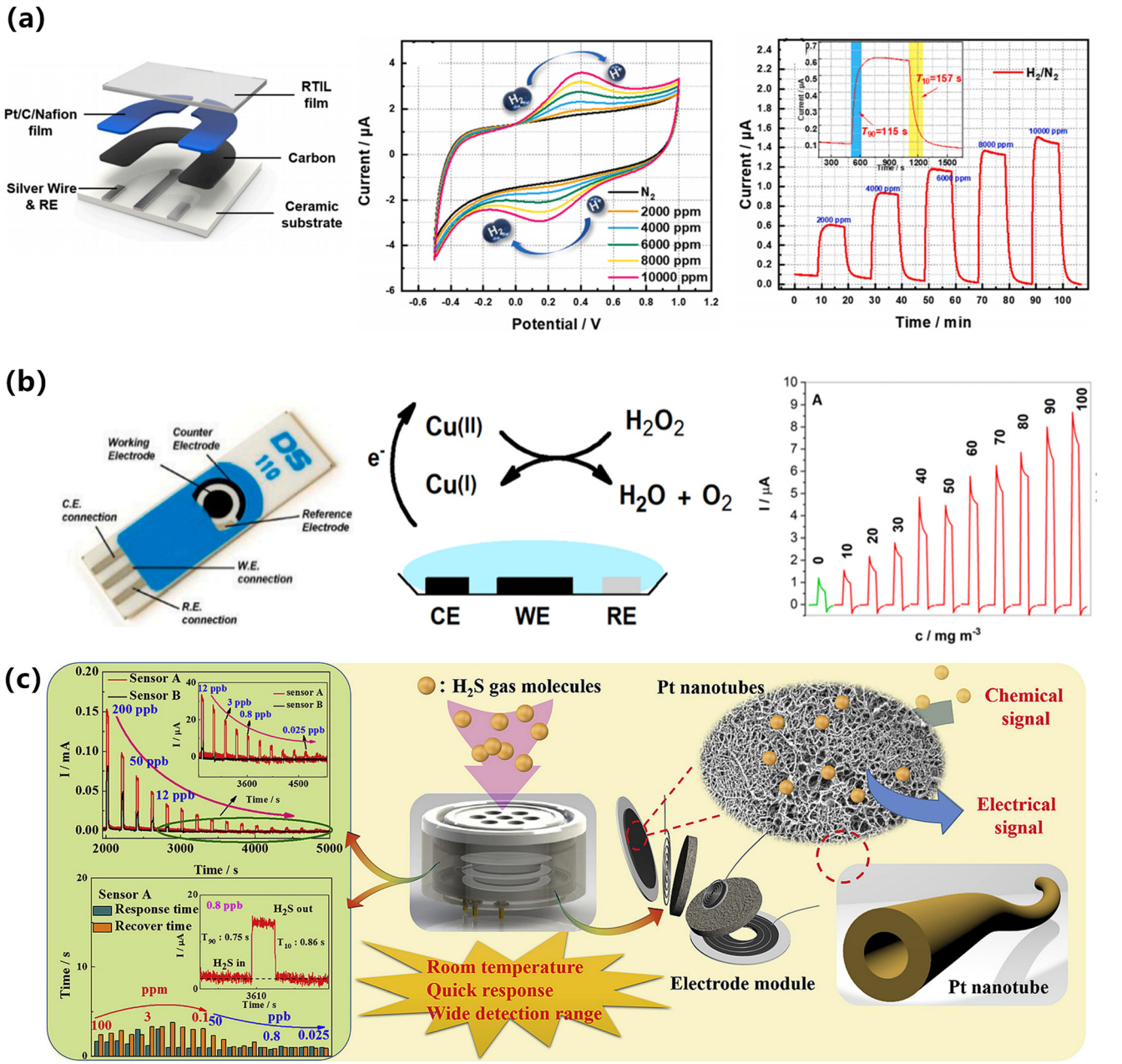

Fig. 4 (a) Schematic diagram of the hydrogen sensor modified with Pt/C/Nafion and the CV and CV detection results. Inset: Magnified cyclic voltammetry region highlighting the oxidation (≈0.4 V) and reduction (≈0.17 V) peaks of hydrogen under anaerobic conditions, confirming the quasi-reversible redox process. Reprinted with permission from ref. 54. Copyright 2022 Elsevier. (b) Schematic diagram of the H_2O_2 sensor based on a copper redox mediator and the CV detection results. Reprinted with permission from ref. 55. Copyright 2023 Elsevier. (c) Schematic diagram and detection results of the high-sensitivity H_2S sensor based on 1D Pt NTs. Inset: Enlarged response/recovery segment of the amperometric curve for 0.8 ppb H_2S, showing ultrafast T90 (0.75 s) and T10 (0.86 s) behavior based on ultrathin Pt nanotube electrodes. Reprinted with permission from ref. 56. Copyright 2021 Elsevier.

real-time monitoring of trace-level ppb H_2S gas at room temperature (Fig. 4c).

Potentiometric electrochemical sensors typically measure open-circuit voltage (OCV) to determine the concentration of target gases by detecting variations in electrode potential.[57] When the sensor is exposed to an environment containing the target gas, the gas molecules diffuse to the WE surface and reach equilibrium. The hydrogen (H_2) between the WE and the RE is then measured using a voltmeter, providing information about the gas concentration.

The working principle of potentiometric sensors is based on the Nernst equation:

$$E = E^0 + \frac{RT}{nF} \ln \frac{[\text{Oxidized species}]}{[\text{Reduced species}]} \quad (1)$$

where:

- E is the electrode potential (V), representing the potential value under specific conditions,
- E^0 is the standard electrode potential (V), which is a constant specific to the electrode reaction under standard conditions (298.15 K, 1 mol L^{-1} concentration, 100 kPa gas pressure),
- R is the gas constant,
- T is the absolute temperature (K),
- n is the number of electrons transferred in the electrode reaction,
- F is the Faraday constant.

Molino *et al.*[58] developed a novel potentiometric CO_2 electrochemical sensor based on a composite membrane of polymer of intrinsic microporosity (PIM-1) and 18-diazabicyclo[5.4.0]undec-7-ene imidazolate (DBU-imidazolate). The high surface area and gas permeability of PIM-1, combined with the chemical affinity and ion-exchange properties of DBU-imidazolate, significantly enhance the CO_2 sensitivity and selectivity. Zhang *et al.*[59] proposed a potentiometric H_2 sensor based on ZnO porous cages. By controlling the amount of cetyltrimethylammonium bromide (CTAB) added during the synthesis of ZnO porous cages, the size and average pore diameter can be tuned to optimize the gas-sensing performance. Under optimal conditions, the sensor exhibited a response signal of 10.6 mV to 0.3 ppm H_2 at 450 °C, demonstrating excellent selectivity and reproducibility.

The working principle of impedance-based electrochemical sensors relies on gas adsorption/desorption and charge transfer processes. In this process, gas molecules adsorb onto the sensing layer of the electrochemical gas sensor, causing changes in the impedance of the sensing layer. EIS is the most commonly used technique for detecting impedance-based electrochemical gas sensors. The interaction of different gases with the sensing material results in varying changes in electrical parameters, allowing for the detection of gas type and concentration through impedance spectral shifts. An impedance-type nitrogen dioxide (NO_2) sensor based on a porous NiO–YSZ mixed conductor layer was designed by Ma *et al.*[60] By adjusting the YSZ/NiO ratio within the porous layer, the morphology and electron-ion conduction properties of the layer can be optimized, thus improving the sensor's response characteristics. Meng *et al.*[61] developed an impedance-type NH_3 sensor using YSZ as a solid electrolyte and $NiFe_2O_4$ as the sensing material. By modulating the $NiFe_2O_4$ loading and calcination temperature, the sensing performance was optimized. This special sensor, operating at 600 °C, demonstrates advantages such as short recovery time, high sensitivity, and good repeatability, while also exhibiting excellent anti-interference capability against CO_2, CH_4, H_2, NO_2, and NO. Zhang *et al.*[62] reported a Pd-doped rGO/ZnO–SnO_2 nanocomposite hydrogen sensor that achieved ultrafast response and recovery times in addition to a very low detection limit. Specifically, the device responded to 100 ppm H_2 within 4 s and recovered within 8 s at 380 °C, with a detection limit as low as 50 ppb. The authors attributed these short time constants to the synergistic effects of reduced graphene oxide (rGO), ZnO–SnO_2 heterostructures, and Pd nanoparticles, which together enhanced charge transfer and surface reaction kinetics. This case highlights that, beyond sensitivity and selectivity, response and recovery times are critical parameters for practical gas sensing, as they determine how quickly a sensor can detect leaks, return to baseline, and be reused. The study demonstrates how heterostructure engineering and catalytic additives can substantially accelerate adsorption–desorption dynamics, thereby underscoring the importance of recovery time in sensor design for safety and healthcare monitoring.

2.4 Fabrication techniques

The fabrication strategies of electrochemical gas sensors play a decisive role in defining electrode geometry, surface morphology, and material distribution, thereby influencing mass transport, charge transfer, and catalytic activity. Beyond simple deposition, these techniques also enable purposeful electrode pattern design, which is increasingly recognized as a key determinant of sensitivity, selectivity, and long-term stability in healthcare-oriented sensors. Among the diverse approaches, photolithography, screen printing, inkjet printing, and spray coating are the most widely employed, each offering unique advantages in resolution, scalability, and compatibility with flexible substrates.

Photolithography provides sub-micrometer resolution and wafer-level uniformity, making it indispensable for the fabrication of interdigitated electrodes (IDEs) and multiplexed sensing arrays. By integrating functional films on lithographically defined IDEs, reproducible current paths and low baseline drift can be achieved, which is crucial for miniaturized electrochemical gas sensors. Belal *et al.*[63] reported spray-printed ZnO thin films onto lithographic IDEs, demonstrating a remarkable NO_2 response of 5298% at 100 ppm and 150 °C. Similarly, functionalized MWCNTs@ZnO composites deposited on lithographic IDEs exhibited room-

temperature NO_2 sensing with 80% response and fast dynamics, underscoring the synergy between high-resolution patterning and spray deposition.[64]

Screen printing is one of the most mature and scalable approaches, widely used for printing working, counter, and reference electrodes onto ceramic or polymer substrates. Its main advantages include low cost, high throughput, and the ability to handle a broad range of inks. Belal *et al.*[65] systematically reviewed the progress of screen-printed gas sensors, highlighting their integration with hybrid processes such as spin coating, drop casting, and inkjet printing, and discussing their potential coupling with IoT, AI, and self-powered technologies to expand application fields. Despite limitations in resolution, screen printing remains a key technology for fabricating disposable and flexible electrochemical sensors.

Inkjet printing offers maskless, digital deposition with high spatial precision, enabling selective modification of electrodes. Belal *et al.*[66] developed a layer-by-layer inkjet-printed δ-MnO_2/graphene hybrid IDE platform, achieving stable flexible micro-supercapacitors with controlled porosity and conductivity. In another study, Bayoumy *et al.*[67] employed microdrop inkjet printing of graphene/GO inks to fabricate interdigitated supercapacitors, obtaining high areal capacitance (195.1 F m^{-2}) and long cycling stability, which highlights the role of IDE finger dimensions in enhancing ion transport. Taulo *et al.*[68] further demonstrated that inkjet printing of SnO_2/NS-rGO nanocomposites onto flexible IDEs enabled low-temperature CO detection (response 13.4 at 110 °C, compared to 1.88 for pristine SnO_2 at 230 °C), with fast response/recovery and mechanical robustness under bending, illustrating its potential for wearable gas sensors.

Spray-printed methods are effective for rapidly producing porous and large-area sensing layers on both rigid and flexible substrates. Belal *et al.*[63] fabricated ZnO nanosheet films *via* spray printing on lithographic IDEs, which exhibited high NO_2 sensitivity and good reproducibility. In a related work, functionalized MWCNTs@ZnO composites deposited by spray printing demonstrated stable NO_2 detection at room temperature with fast dynamics, emphasizing the ability of spray coating to integrate functional nanomaterials with patterned electrodes.[64] Compared with other methods, spray printing is particularly advantageous in forming hierarchical porous films that promote gas diffusion and catalytic activity.

Importantly, the true impact of these fabrication routes lies in their ability to engineer electrode patterns. Interdigitated structures with optimized finger width and spacing minimize diffusion barriers and reduce ohmic losses, enabling faster response and higher sensitivity. Porous or 3D microstructures achieved through spray or inkjet techniques expand the electrochemically active surface area, thereby lowering detection limits. Moreover, selective printing (*e.g.*, depositing catalytic or selective membranes only on the WE) enhances gas selectivity in complex mixtures. Recent advances clearly show that purposeful electrode pattern design, empowered by appropriate fabrication strategies, is essential for translating electrochemical principles into robust, miniaturized gas sensors for next-generation healthcare and environmental monitoring.[66,69]

3. Development of smart electrochemical gas sensors

3.1 Sensors with IoT

Devices developed based on IoT have been successfully applied across various fields, yielding promising results. Chen *et al.*[70] reported a method for implementing a vital signs health monitoring system using IoT technology. This system was applicable in medical settings, including hospitals, and had achieved an accuracy rate exceeding 99% in health status assessments. Chakraborty *et al.*[71] developed an open-source, IoT-based detection system for asthma patients, which consisted of two parts: the frontend integrated harmful gas sensors with environmental monitors, while the backend connected IoT technology with a software database. The reliability of the system's performance was confirmed by comparing its experimental data with that from commercially available devices. As the digitalization era and Industry 4.0 continue, monitoring technologies based on sensors have become increasingly common in the mining industry.[72] In hazardous work environments, integrating modules like toxic gas sensors into personal protective equipment (*e.g.*, helmets) offers a highly effective application of smart sensors. These devices continuously collect real-time environmental data and monitor workers' health, transmitting the data *via* Bluetooth to a control module outside the mining area. This facilitates timely hazard warnings, allowing workers to take preventive measures and avoid injuries.[73] Ammonia (NH_3), a hazardous and toxic atmospheric pollutant, poses significant health risks when exposed to high concentrations. Zhuang *et al.*[74] proposed a high-sensitivity flexible NH_3 detection wireless system based on polyaniline/multi-walled carbon nanotube composites, designed for real-time monitoring in an IoT environment. This method used a composite of polyaniline and multi-walled CNT as the sensing material, coated onto silver interdigitated electrodes, and placed on a polyethylene terephthalate (PET) substrate. The system integrated a microcontroller with Wi-Fi capability, forming a flexible electronic system. This solution addressed the integration challenges of flexible electronic systems.

Technological advances have enabled the mass production of inexpensive electrochemical sensors capable of measuring air pollution gas concentrations with relatively high accuracy. IoT modules are ideal for integration into these low-cost sensors, and deploying multiple sensor nodes in high-risk environments or urban areas can facilitate large-scale gas detection networks.[75,76] However, traditional client–server and cloud-based data management systems are vulnerable to single points of failure, centralized data management issues, and other system weaknesses. To address these challenges,

Gao's team[77] developed a new IoT-based monitoring system (WG-IoT-MS) that effectively monitors and simulates CO_2 and N_2O emissions in agricultural water bodies, reducing monitoring costs by approximately 60%. This advancement tackled the challenges of cost and portability in simultaneously monitoring water quality and greenhouse gas emissions in rice paddy fields.

3.2 Sensors with self-powered technologies

With the advancement of flexible electronics, the miniaturization and lightweight nature of wearable gas sensors have opened new possibilities for portable gas detection and health monitoring systems, focusing on integration and smart functionalities. However, the reliance on external power sources limits their portability and wearability. Moreover, the rapid expansion of IoT has resulted in sensor networks that are numerous, decentralized, and operate independently, leading to challenges such as high energy consumption and maintenance difficulties in traditional battery-powered systems. To address these issues, integrating self-powered/self-driven technologies into sensors offers a promising solution. By harnessing abundant environmental energy sources—such as mechanical, solar, thermal, wind, and ocean energy—these systems enable autonomous detection of target gases, eliminating the need for external power. This approach paves the way for the development of efficient, energy-saving, and sustainable gas sensors. The core of self-powered devices lies in energy harvesting technologies, which convert ambient energy into electrical power. Significant advancements have been made in various energy harvesting methods, including photovoltaic generation,[78] thermoelectric generators,[79,80] mechanical energy harvesters,[81,82] biofuel cells (BFCs)[83,84] and radio frequency energy harvesters.[85,86] Among these, the invention of TENGs has provided a breakthrough for the development of next-generation self-powered gas sensors.[87] Based on the coupling effect of triboelectric charging and electrostatic induction, TENGs can convert mechanical energy into electrical signals. When positive and negative triboelectric materials come into contact and then separate, TENGs generate an alternating current (AC) flow from one electrode to another through an external circuit. There are four fundamental working modes of TENGs, as shown in (Fig. 5a).[88] Currently, self-powered gas detection systems utilizing TENGs can be categorized into two types based on the role of the TENG. The first type is a separated gas sensor driven by TENG, which uses the load matching effect of the TENG, where the TENG and gas sensor function as the power and sensing units, respectively. The second type involves a TENG serving both as an energy generator and a gas sensor, achieved by employing a sensing functional film with both gas-sensing and triboelectric properties. When target gas molecules adsorb onto the film, the chemical potential on the surface changes, directly altering the surface charge density of the triboelectric material. Consequently, the output electrical signal of the TENG varies in response to the type and concentration of the detected gas.

Polymers such as PTFE, nylon, and latex are commonly used as triboelectric film materials. For example, in the TENG-powered NH_3 sensor proposed by Wang *et al.*,[89] PTFE and nylon were used as the two triboelectric films (Fig. 5b). Another NH_3 sensor was powered by a TENG based on PTFE and latex.[90] Su *et al.*[91] developed a self-powered gas sensor array driven by a Maxwell displacement current (Fig. 5c), designed for wireless, passive respiratory analysis and exhaust emission monitoring. The relative rotation between PTFE rotator and nylon stator generates a time-varying electric potential in the entire space with a period of $\pi/2$, resembling the displacement effect. Due to their softness and flexibility, nanofiber materials are also commonly used as triboelectric layers in wearable gas sensors. Sardana *et al.*[92] synthesized an electrospun TENG using highly electronegative and conducting MXene nanofibers (NFs) paired with biodegradable cellulose acetate NFs (CA-NFs) as triboelectric layers, achieving a sufficient power density ($\sim$1361 mW m^{-2} $M\Omega^{-1}$). By embedding a triboelectric pair in the smart insole, the TENG harvests kinetic energy from footfall motion to power an MXene/TiO_2/cellulose-NFs heterojunction-based sensor and LED indicators for NH_3 leakage detection (Fig. 5d). Wang *et al.*[93] fabricated a wind-driven TENG based on poly(vinyl alcohol)/Ag nanofiber films for human respiration and movement stimulation monitoring (Fig. 5e). By integrating four TENGs with a high-performance $Ti_3C_2T_x$ MXene/tungsten oxide nanofiber-based NO_2 gas sensor, this multifunctional self-powered detection system can trace the source of harmful gases. Additionally, Wang *et al.*[94] constructed a liquid–solid TENG with ECTFE film and ionic hydrogel electrodes to harvest wave energy for marine environmental monitoring, derived from the contact electrification between water and ECTFE (Fig. 5f).

For a self-powered active gas sensor that functions both as an energy generator and a gas sensor, at least one of the triboelectric layer materials or electrode materials must possess gas-sensing properties. Wang *et al.*[95] introduced a respiration-driven TENG using $Ti_3C_2T_x$ MXene/NH_2-MWCNTs for self-powered detection of exhaled gas and disease diagnosis. The MXene/NH_2-MWCNTs composite, serving as both the friction layer and electrode of the TENG, is sensitive to formaldehyde (HCHO) gas, resulting in varying output voltages when exposed to different HCHO concentrations (Fig. 5g). To improve the output sensitivity of triboelectric respiration sensors (TRSs), Liu *et al.*[96] designed a lever-type TRS (Fig. 5h). By adjusting the length ratio of the power arm to the resistance arm, they modulated the contact-separation distances between dielectrics, resulting in a TRS that exhibits flow sensitivity during oral/nasal respiration. Additionally, an *in situ* self-assembled Fe^{2+} doped polypyrrole (FPPy) sensing film was selected as one of the back electrodes of the triboelectric

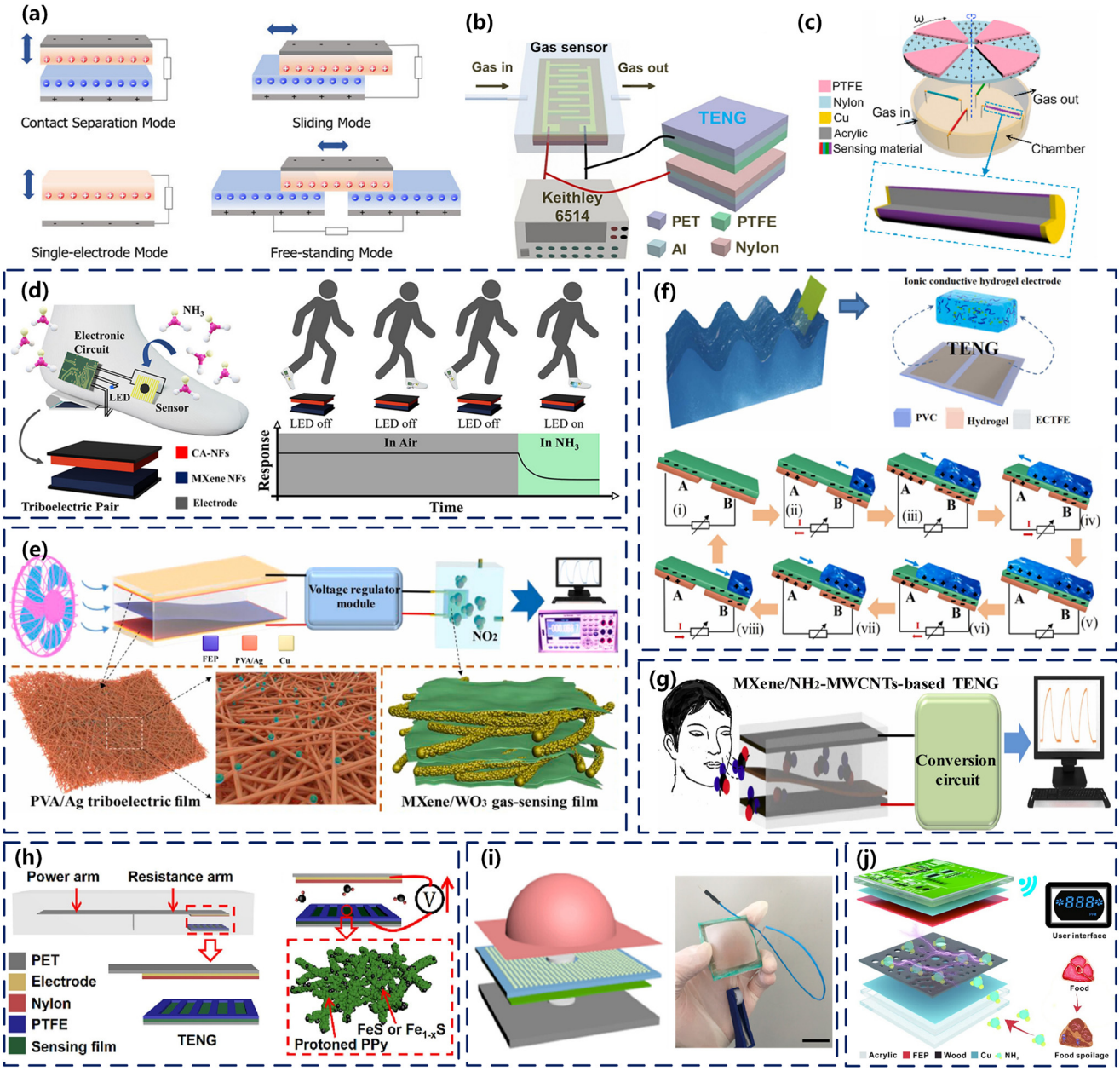

Fig. 5 (a) Four working modes of TENG. Reprinted with permission from ref. 88. Copyright 2022 Wiley. (b) and (c) TENGs utilizing PTFE and nylon as triboelectric films. Reprinted with permission from ref. 89 and 91. Copyright 2021, 2023 Elsevier. (d) Mxene Nfs and CA-NFs based TENG integrated into a smart shoe insole. Reprinted with permission from ref. 92. Copyright 2022 American Chemical Society. (e) PVA/AG NFs based wind-driven TENG. Reprinted with permission from ref. 93. Copyright 2021 Elsevier. (f) Wave-driven TENG with ECTFE film and ionic hydrogel electrodes. Parts (i)–(viii) show the charge transfer mechanism of TENG. Reprinted with permission from ref. 94. Copyright 2022 Elsevier. (g) Respiration-driven TENG using $Ti_3C_2T_x$ MXene/NH_2-MWCNTs. Reprinted with permission from ref. 95 Copyright 2022 Elsevier. (h) Lever-type triboelectric respiration sensors. Reprinted with permission from ref. 96. Copyright 2023 Elsevier. (i) Alveolus-inspired membrane sensor. Reprinted with permission from ref. 97. Copyright 2020 American Chemical Society. (j) TENG-based wireless gas sensor system reprinted with permission from ref. 98. Copyright 2021 Elsevier.

layers due to its selective reaction between Fe^{2+} and H_2S. Consequently, the developed TRS is also capable of detecting H_2S in exhaled gases. Su *et al.*[97] developed an alveolus-inspired membrane sensor (AIMS) that converts the mechanical inflating and deflating of gases in a latex film into electrical signals (Fig. 5i). When combined with gas-sensing materials, it enables both NO_2 detection and continuous monitoring of breathing behavior. Another example is the TENG-based wireless gas sensor system (TWGSS)[98] used for food quality evaluation (Fig. 5j). The NH_3-sensing conductive wood, chemically modified and incorporated with CNTs, exhibits excellent mechanical flexibility and gas adsorption capacity due to its porous structure.

Similar to TENGs, piezoelectric nanogenerators (PENGs) are widely used technologies for converting mechanical energy into electrical energy. PENG relies on the property of piezoelectric materials to generate electric fields upon deformation. This piezoelectric effect is suitable for self-powered sensor applications in dynamic environments with vibrations or human motion. To optimize energy harvesting, piezoelectric materials are often integrated with flexible substrates to form microelectromechanical systems (MEMS). In the study by Zhang *et al.*,[99] a flexible piezoelectric nanogenerator was developed using a 2D single-layer MoS_2 flake on PET. The Au-$MoSe_2$ composite-based ammonia sensor with the MoS_2 PENG exhibited an enhanced response (V_a/V_g = 29 at 100 ppm NH_3). Furthermore, the sensor demonstrated a rapid response and recovery time of 18 s and 16 s, respectively, when exposed to 20 ppm NH_3. Photovoltaic energy harvesting converts light into electrical energy *via* the photoelectric effect, where light generates electron–hole pairs in a photoelectric semiconductor material that are separated by an internal electric field, producing current. In low-light environments, the generated energy is typically stored in supercapacitors or batteries to ensure continuous sensor operation. In the work of Niu *et al.*,[100] a photovoltaic self-powered NO_2 gas sensor was developed using a vertical MoS_2 (n-type)/GaSe (p-type) heterojunction. The sensor demonstrated outstanding performance in detecting NO_2, including rapid response and recovery times and high selectivity in both biased and self-powered modes. Notably, the limit of detection (LOD) for NO_2 was as low as 20 ppb in the fabricated photovoltaic self-powered gas sensor. Thermoelectric energy harvesting is based on the Seebeck effect, where a temperature gradient across a thermoelectric material drives charge carriers from the hot end to the cold end, creating a potential difference that results in current generation.

3.3 Sensors with machine learning

ML has emerged as one of the fastest-growing technologies in recent years, typically comprising four stages: data collection, model building, training, and evaluation. ML models can be classified into supervised and unsupervised categories, based on whether the model relies on labeled data during the learning process. In supervised learning, training data is used to model and train classifiers, allowing them to recognize feature labels associated with the objects of interest. Common classification models include support vector machines (SVM),[101,102] decision trees (DF),[103,104] *k*-nearest neighbors (KNN),[105,106] artificial neural networks (ANN),[107,108] random forests (RF),[109,110] and others. Unsupervised learning, on the other hand, involves training the model without labeled data or target outputs. The goal is to uncover hidden structures, patterns, distributions, or relationships within the data, without relying on label information. Common unsupervised learning algorithms include *K*-means,[111,112] hierarchical clustering,[113] Gaussian mixture models (GMM),[114,115] principal component analysis (PCA),[116,117] and others.

Current commercial VOC detectors suffer from cross-sensitivity and low repeatability. The introduction of ML methods allows for feature extraction from the data to classify different types of VOCs and their mixtures. Huang *et al.*[118] proposed a species-selective detection method for VOCs using electrochemical cells based on ionic liquid (IL) electrolytes. Linear discriminant analysis (LDA) was used to extract and classify the measured voltammograms. Zhang's team[119] developed a wearable mask for detecting and identifying VOCs. During the analysis and identification steps, PCA and KNN were employed for dimensionality reduction, feature extraction, VOC recognition, and concentration prediction, with results demonstrating high accuracy (Fig. 6a). Tombel *et al.*[120] applied five supervised ML algorithms to predict VOC classification using an initial dataset: KNN, RF, SVM, logistic regression (LR), and ANN. They found that RF and KNN models showed higher accuracy, and that selecting the simplest features from the steady-state stage was sufficient for gas classification. Similarly, Gupta *et al.*[121] found that RF and KNN models demonstrated better accuracy in predicting normal breathing *versus* respiratory failure across multiple model comparisons.

ANNs are a ML approach that enables the learning and classification of data patterns. The multi-layer perceptron (MLP) is a type of feedforward neural network model that maps multiple input datasets to a single output dataset. Chen *et al.*[122] developed an electronic nose system for online breath analysis based on a graphene sensor array and the MLP model. This system used the MLP model to perform pattern recognition of the responses of different gases on the graphene array, demonstrating that the method could effectively detect and analyze volatile compounds in exhaled breath. Li *et al.*[123] designed a collaborative strategy based on sensor integration and ML algorithms for the precise detection of NH_3 and NO_2 gases. They employed the BP-NN algorithm for qualitative gas analysis and used partial least squares (PLS) regression analysis for quantitative prediction (Fig. 6b). Besides, Sun *et al.*[124] conducted an analysis and comparison of various artificial intelligence algorithms for the real-time monitoring of volatile compounds in urine. They found that the convolutional neural network (CNN) model performed best in extracting local features, mining global training features, and classifying spatial vectors. Liu *et al.*[125] proposed a feasible approach for selectively detecting chemical mixtures using a single non-selective sensor. By applying ML models, specifically a recurrent neural network (RNN) with gated recurrent units (GRU), the study successfully learned the response signals of a C_2H_2–C_2H_4 mixture, enabling the prediction of mixture composition from overlapping signals, thus providing new ideas for intelligent detection.[126–128] Heng *et al.*[129] designed an artificial intelligence-assisted sensor system for detecting

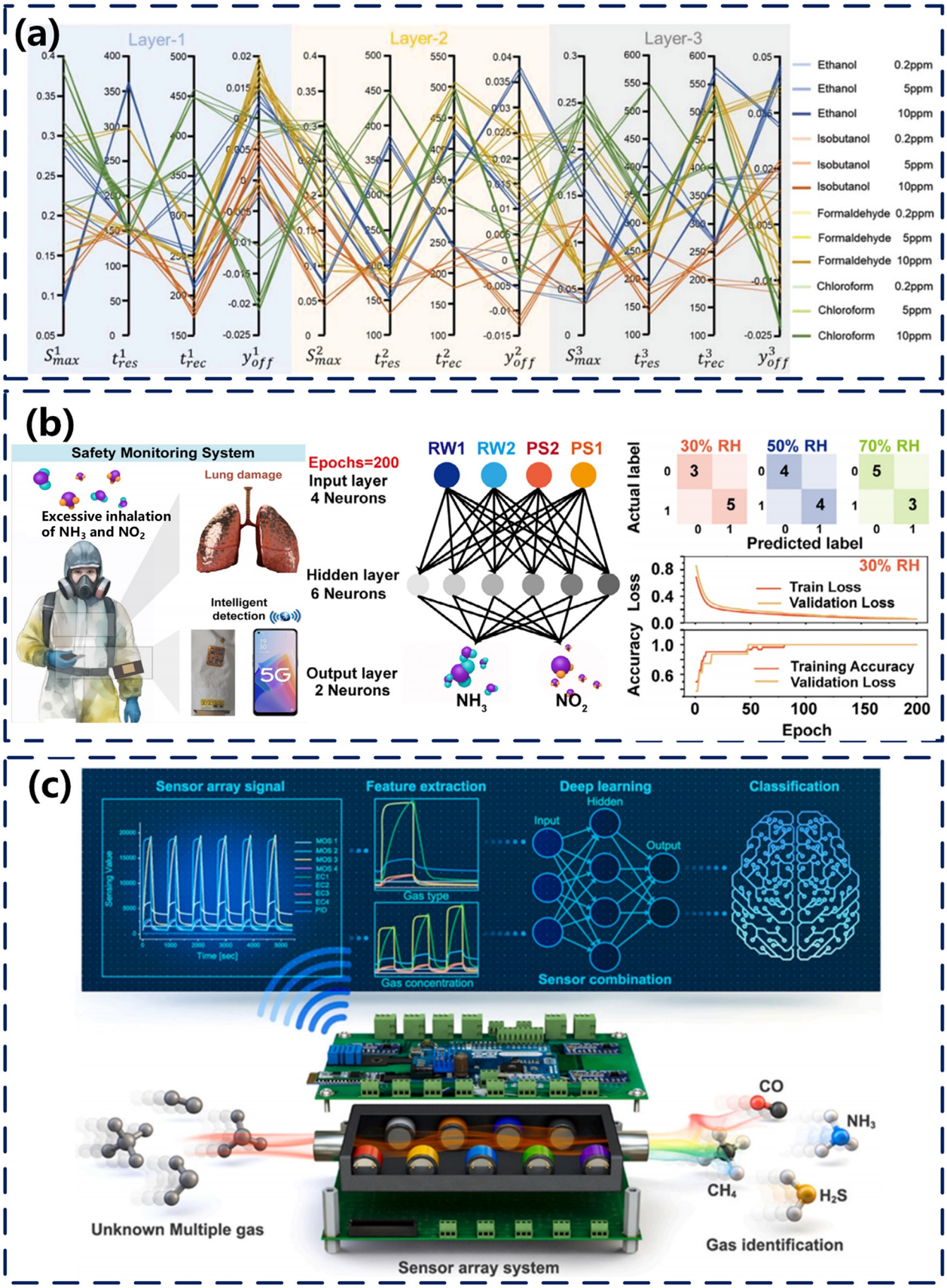

Fig. 6 (a) Parallel coordinate plots of 12 parameters extracted from all VOC gas response measurements. Reprinted with permission from ref. 119. Copyright 2024 Wiley. (b) Safety monitoring system and the BP-NN network architecture.[123] (c) Schematic of the hybrid sensor detector combined with ML algorithms. Reprinted with permission from ref. 132. Copyright 2024 Elsevier.

acetone and ethanol. The sensor array, consisting of various metal oxide (MOx) sensors, was exposed to acetone and ethanol to generate a dataset for training and testing a multi-input CNN. This study confirmed that the deep learning model CNN is more effective at capturing dynamic interactions between sensors and acetone and ethanol compared to traditional ML methods such as LDA, KNN, and SVM.

ML techniques can be applied not only in the data post-processing stage to compensate for sensor performance deficiencies and improve the selectivity of target gases, but also in the pre-processing stage to address interference caused by environmental factors. The performance of GO-based VOC sensors, for example, is influenced by changes in relative humidity (RH) in the surrounding environment. To mitigate RH interference, Lim *et al.*[130] compared two deep learning networks, transformer and LSTM, and found that both models could accurately predict a 1% change in relative humidity, with the transformer model performing better. This technology helps calibrate gas sensors developed in the laboratory within a typical humidity range. Additionally, detecting target gases in open environments requires careful consideration of the measurement environment, as the physical properties of gas molecules are highly influenced by external factors such as wind speed. To address the multi-condition gas classification problem, Lee *et al.*[131] designed a novel deep learning network called 'MCGCN', which uses a shared feature extraction module (SFEM) for efficient feature extraction and a new loss function consisting of combined classification loss and individual condition loss for training. It achieves high accuracy (99.15% ± 0.41) while reducing the model parameters by a factor of 15 compared to previous methods. In another study, gas sensor arrays combined with ML models show significant development potential. Ku *et al.*[132] proposed combining three different sensor principles: semiconductor metal oxide (SMO) sensors, electrochemical (EC) sensors, and photoionization detection (PID) sensors to create a hybrid sensor array. By integrating ML, this array can rapidly respond to and identify hazardous gas leakage environments in chemical plants. This research highlights the deep integration of sensor technology and ML, offering new ideas for the development of intelligent sensing systems. It is significant for advancing sensor technology and promoting the application of artificial intelligence in various fields (Fig. 6c).

4. Applications of smart electrochemical gas sensors

4.1 Air monitoring

Air pollution presents a significant threat to both the environment and public health. Traditional air quality monitoring stations, due to their costly equipment, are typically limited to small areas and lack high-density spatial resolution. Recent advances in low-cost sensors and IoT have enabled the large-scale deployment of sensor networks. Additionally, the integration of lightweight algorithm models can mitigate sensor aging, allowing for real-time and long-term air pollution monitoring.

Nitrogen dioxide (NO_2) is a major component of air pollution, primarily resulting from industrial emissions, transportation, and residential combustion processes. Long-term exposure to NO_2 can lead to respiratory diseases such as bronchitis, pulmonary edema, and asthma. Therefore, highly sensitive and selective NO_2 sensors are crucial for air quality monitoring. Zhang *et al.*[39] presented an ultra-sensitive NO_2 sensor that operates at room temperature (RT), based on $K_2Fe_4O_7$ solid electrolyte and Ni-MOF|N_2 sensing electrode (SE). The sensor operates on the mixed potential principle (MPSE), where the potential signal is determined by the electrochemical reaction of the target gas. By controlling O_2 vacancies and the unsaturated coordination state of Ni ions, the sensor's selectivity for NO_2 is enhanced, providing a 31-fold improvement over NO. The sensor is integrated into an IoT terminal, enabling remote monitoring and information sharing. Ali *et al.*[133] proposed a low-cost sensor node based on LoRaWAN, capable of measuring CO, NO_2, and particulate matter (PM), calibrated using ML to improve accuracy. The development of such low-cost electrochemical sensors offers new possibilities for air quality monitoring. While these sensors may not match the accuracy of traditional devices, their low cost and potential for large-scale deployment make them valuable complements to conventional monitoring systems. However, low-cost sensors are not only limited by inherent sensing accuracy but also affected by environmental factors (such as temperature and humidity) and sensor drift over time, leading to a decline in measurement accuracy. As a result, research on various calibration methods has become a key research focus in recent years.[30,134] Christakis and colleagues[75] investigated the effect of sensor aging on measurement accuracy and proposed a correction formula to address this issue. The team set up a wireless sensor network (WSN) consisting of three sensor nodes in downtown Athens, Greece, with each node equipped with electrochemical sensors for monitoring NO_2 and ozone (O_3) concentrations. The sensor data were compared with official monitoring stations to assess accuracy. The team continued to focus on optimizing low-cost electrochemical air quality sensors for measuring O_3 and NO_2, proposing a new correction method based on quadratic polynomial regression the following year. The corrected data showed better alignment with official reference instrument data, enhancing the feasibility of low-cost sensors in real-world applications.[135] Interestingly, portable environmental sensors can also serve as diagnostic tools for patients with COPD.[136] COPD is a chronic disease that affects the respiratory system, and its symptoms can be exacerbated by environmental factors such as air pollution. Timely prediction of COPD symptom deterioration can help doctors make more accurate diagnoses. A prediction model combining probabilistic latent component analysis (PLCA) and linear dynamic systems (LDS), known as PLCA-LDS, was

proposed by the Kolozali team to predict changes in patient symptoms. Experimental results showed that the new model achieved a 4–20% improvement in accuracy over the RF model in predicting COPD symptoms. This study is the first to demonstrate the feasibility of using personal air pollution exposure data to predict COPD symptoms and highlights the potential of portable sensors and ML technologies in remote health monitoring. In addition, chemical plants, underground mines, waste treatment facilities and other places are often accompanied by various toxic and harmful gases. Fazio *et al.*[137] proposed and developed a self-powered smart shirt, which integrates multiple wearable sensors

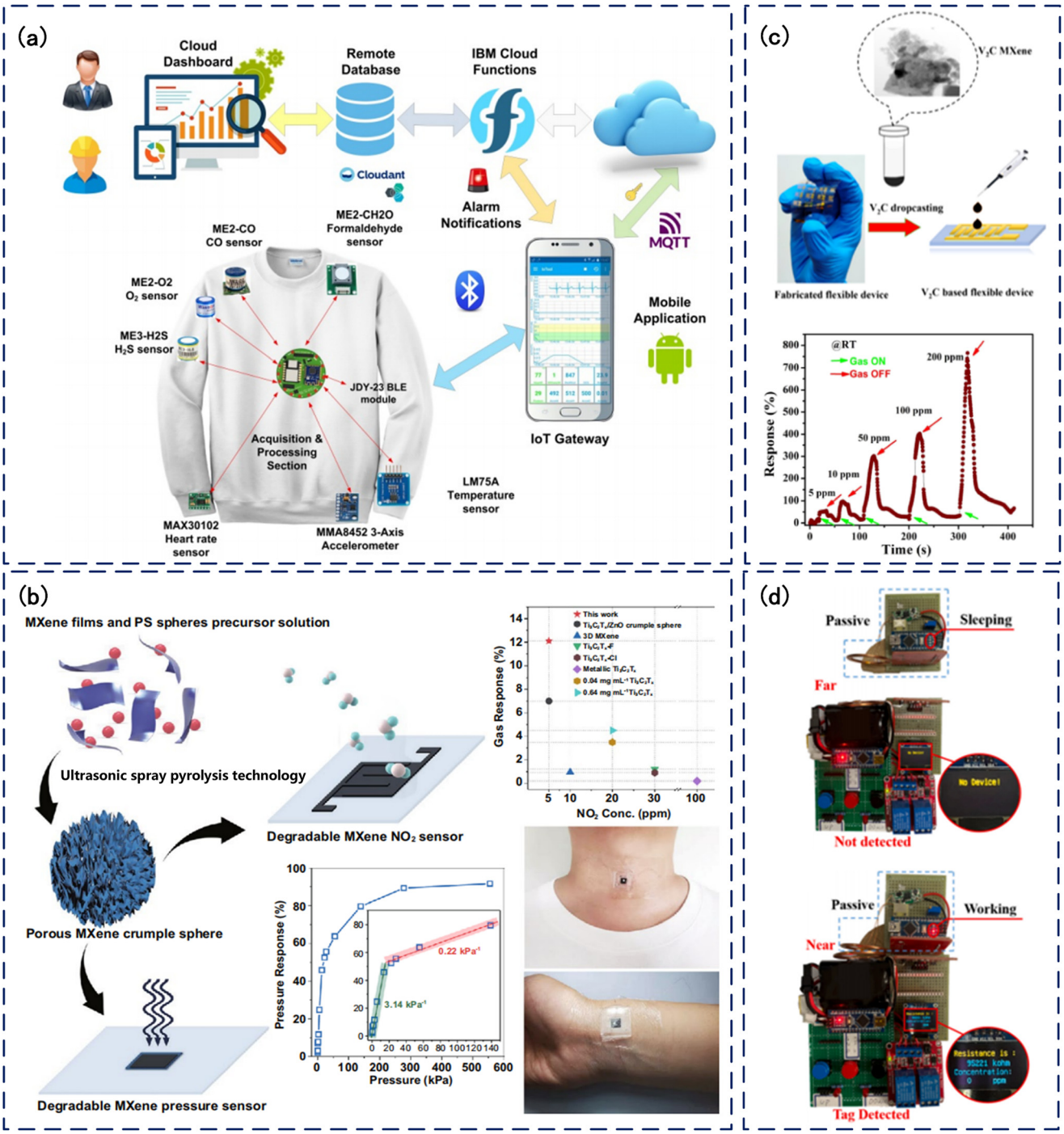

Fig. 7 (a) The deployed monitoring system relying on the proposed wearable device.[137] (b) The transient all-MXene NO_2 and pressure sensors and the photo of the pressure sensor on the skin. Inset: Photograph of the wearable sensor attached to the human wrist during measurement.[138] (c) The vanadium carbide MXene based flexible and room temperature toluene gas sensor. Reprinted with permission from ref. 139. Copyright 2024 American Chemical Society. (d) Non-working state and working state of the composite device. Reprinted with permission from ref. 143. Copyright 2023 Elsevier.

capable of monitoring workers' physiological indicators. The smart shirt transmits data to a smartphone *via* BLE modules, with the smartphone acting as an IoT gateway to upload data to the IBM Cloud platform for storage, processing, and visualization (Fig. 7a).

In order to better distinguish and quantitatively detect toxic gases, it is necessary to pay attention to the progress of sensitive materials in recent years, such as graphene/GO-based materials, CNTs, MOFs, and conducting polymers. Particularly, MXene-based gas sensors have demonstrated outstanding gas sensing performance owing to their unique two-dimensional structure and abundant surface functional groups. MXene-based gas sensors can exhibit excellent performance at room temperature. For example, Yang *et al.*[138] developed a full MXene transient NO_2 sensor based on three-dimensional porous wrinkled MXene spheres, which showed a response of up to 12.11% for 5 ppm of NO_2 at room temperature, with a detection limit as low as 50 ppb and excellent reproducibility and selectivity. Furthermore, the flexible properties of MXene materials offer broad application prospects in wearable gas sensors (Fig. 7b). Karmakar *et al.*[139] reported a flexible toluene gas sensor based on V_2C MXene, which showed a 77.5% response to 200 ppm of toluene at room temperature. This flexible sensor can be integrated into wearable devices to monitor harmful gas concentrations in real-time, thereby protecting human health. The lightweight nature and high mechanical strength of MXene materials make them ideal for portable gas sensors, enabling real-time monitoring in complex environments. Lastly, the multifunctionality and tunability of MXene materials offer new directions for developing multifunctional gas sensors (Fig. 7c). Gorbounov *et al.*[140] introduced an outdoor mine atmospheric monitoring system based on LoRa wireless technology, using MEMS gas sensors for real-time monitoring of harmful gases such as NO, NO_2 and CO. By integrating MXene materials with wireless communication technology, remote and real-time gas monitoring can be realized, significantly improving the portability and practicality of the monitoring system.

Trimethylamine (TMA) is a VOC with a strong fishy odor. Prolonged exposure can irritate the eyes, nasal cavity, and skin, and may affect the nervous system.[141,142] However, current TMA sensors often require high-temperature heating to improve sensitivity, presenting challenges in energy consumption and safety. Li *et al.*[143] designed a passive near-field communication (NFC) tag-type TMA gas sensor based on WO_3/MXene composite materials, achieving high-sensitivity detection at room temperature. The research team utilized the MXene layered structure to increase the reactive active sites of WO_3 nanoparticles and form Schottky junctions, thereby enhancing the selectivity and response speed of WO_3 to TMA. NFC technology is used to develop a non-contact gas detection device that does not require an external power supply, improving the safety and convenience of detection (Fig. 7d).

Indoor air pollution is now ranked among the top five environmental public health risks that contribute to morbidity and mortality globally, particularly since indoor pollutant concentrations can be several times higher than those found outdoors.[134,144,145] Consequently, monitoring indoor environments is a vital application for intelligent gas sensors. Traditional air quality monitoring methods typically rely on expensive instruments and complex laboratory analysis, which cannot meet the demands for portability, low cost, and low power consumption. To address these challenges, González *et al.*[146] proposed a LoRa-based sensor network that integrates commercial gas sensors and graphene-based chemical resistive sensors to detect VOCs, CO, and NO_2, providing real-time air quality monitoring. The commercial sensor (BME680) computes the indoor air quality index using built-in algorithms, although it cannot accurately detect oxidizing gases like NO_2. The graphene sensor, on the other hand, rapidly responds to changes in NO_2 concentrations, making it suitable for detecting gas leaks. Furthermore, the LoRa network offers excellent scalability and communication performance, allowing for the easy addition of new nodes to the network without modifying gateway configurations. These sensor networks are ideal for indoor air quality monitoring and early gas leak detection.

HCHO is another significant indoor pollutant that raises health concern. The World Health Organization classifies it as a carcinogen when individuals are exposed to concentrations above 0.08 ppm over an extended period.[147] Zhang *et al.*[148] proposed a Cr-doped Pd-based electrochemical HCHO sensor, which exhibits a detection range one order of magnitude higher and significantly better anti-interference capabilities compared to conventional sensors. Most importantly, this HCHO sensor is suitable for both indoor and outdoor environmental monitoring when integrated into WSNs or handheld devices. Wang *et al.*[95] designed a multifunctional self-powered system based on TENG. The team prepared a composite based on amino-functionalized multi-wall carbon nanotubes (NH_2-MWCNTs). The composite material is used as both a friction layer and an electrode to improve the sensitivity of the sensor to formaldehyde. Experiments have compared the response of a variety of gases (such as methanol, acetone, ammonia, benzene), showing a higher selectivity for formaldehyde. It provides innovative design scheme and experimental evidence for self-powered gas sensor and respiratory behavior monitoring. The use of visible light assisted strategy is an innovative idea. Based on this method, Liu decorated Pd on titanium dioxide to enhance its photocatalytic performance.[149] The sensor showed good linear response in the concentration range from 80×10^{-9} to 50×10^{-6}. Under visible light irradiation, the sensor not only doubled the response to formaldehyde, but also changed little in response to other interfering gases (such as NH_3, acetone, benzene, *etc.*), thus improving the gas selectivity. Additionally, several studies aim to

integrate individual gas sensors into a network for comprehensive indoor air quality monitoring in smart homes. Marques and Pitarma[150] presented an IoT system for real-time indoor air quality monitoring called iAir. This system features a hardware prototype for environmental sensing and a web/smartphone interface for data access. The collected data is transmitted to an open-source IoT platform that provides an API for cloud storage and retrieval.

4.2 Breath analysis

In recent years, the rapid development of breath detection technologies has brought exhaled breath to the forefront as a novel and promising biological sample, gaining increasing recognition as a valuable tool for the early diagnosis and monitoring of diseases. Over 2000 VOCs have been found in exhaled gases, providing a wealth of information about overall health.[2] This offers great potential for disease biomarkers to be sampled non-invasively through respiratory biopsy.[151] Moreover, a growing body of evidence indicates that the relationship between diseases and exhaled VOCs is highly complex. Most diseases are not characterized by a single compound, but rather by a complex of multiple VOCs, many of which may overlap across different pathological conditions. Moura *et al.*[152,153] summarized representative examples of diseases and their related VOCs, highlighting the diversity of VOCs and the challenges of overlapping labeling. A summary of their key findings is presented in Table 1. This overlap poses a significant challenge for establishing disease-specific diagnostic markers, as relying on a single VOC is often insufficient for accurate discrimination. To overcome this limitation, researchers increasingly focus on identifying unique VOC patterns or multi-marker signatures that, when combined with advanced data analysis, can provide improved specificity.

Recent studies employ sensor arrays combined with machine learning and statistical modeling to capture these complex patterns, thereby improving specificity and reducing diagnostic ambiguity. Recent advances have demonstrated the potential of combining multi-sensor arrays with machine learning algorithms to improve the accuracy of VOC-based disease detection. Lee *et al.*[11] developed a breath analysis system for the early diagnosis of lung cancer, integrating a gas sensor array with deep learning models. The platform employed nine electrochemical sensors, a semiconductor metal oxide sensor, and a photoionization detector to simultaneously monitor multiple VOCs in exhaled breath. Clinical validation on 181 breath samples (107 lung cancer patients and 74 healthy controls) showed that the system, when coupled with a 1D CNN, achieved an accuracy of 97.8% in distinguishing lung cancer patients from healthy individuals. Importantly, the comparison of different neural architectures (multilayer perceptron, recurrent neural network, and CNN) demonstrated the superiority of CNN for handling high-dimensional VOC data. This study underscores how multi-marker VOC signatures, when analyzed through deep learning, can overcome the limitations of single-compound analysis and significantly enhance the specificity of breath-based diagnostics. The novel electronic nose (e-nose) system developed by Vadera and Dhanekar[154] represents a promising technology for non-invasive diagnostic applications, particularly in the analysis of exhaled breath. By combining sensor arrays with advanced machine learning (ML) algorithms, e-nose systems can classify and predict the presence of specific VOCs, which act as biomarkers for various diseases. Additionally, the use of IoT-enabled prototypes, such as those incorporating Raspberry Pi

Table 1 Exhaled breath biomarkers of VOCs corresponding to five diseases[152]

Disease	Volatile organic compounds as exhaled breath biomarkers
Asthma	Acetone, biphenyl, decane, 1,4-dichlorobenzene, 3,6-dimethyldecane, 2,4-dimethylheptane, 1,7-dimethylnaphtalene, 2,4-dimethylpentane, dodecane, 2-ethenylnaphtalene, ethylbenzene, 2-ethyl-4-methylpentanol, hexane, 2-hexanone, 1-isopropyl-3-methylbenzene, 2-methylhexane, 3-methylpentane, 1-(methylsulphonyl)propane, 4,6,9-nonadecatriene, nonanal, nonane, octadecyne, octane, 2-octenal, 2,2,4,6,6-pentamethylheptane, phenylbutene, propanol, tetradecane, 2,6,10-trimethyldodecane, 2,2,4-trimethylheptane, 2,3,6-trimethyloctane, 2-undecanal, *p*-xylene
Chronic kidney disease	Acetone, ammonia, aniline, bicyclo[4.1.0]hepta-1,3,5-triene, 2-butanone, 2-chloroethylester-carbonochloridic acid, 3-chloropropanoylchloride, *o*-cymene, dichloronitromethane, 2,4-dimethylheptane, dimethyl sulphide, ethanol, ethenesulfonyl chloride, *m*-ethylmethylbenzene, 2-ethylpentane, 3-ethylpentane, heptanal, hexanal, iodide cycloheptatrienylium, isoprene, limonene, methane sulfonyl chloride, methanethiol, methylamine, methylene chloride, 2-methylhexane, 3-methylpentane, 6-nitro-2-picoline, nonanal, pentanal, 4-(1-phenyl-2-propenyloxy)-benzaldehyde, 1*H*-pyrazole-4-carbonitrile, 2-pyridinecarbonitrile, 1*H*-pyrrole-3-carbonitrile, silicon tetrafluoride, styrene, toluene, 4*H*-1,2,4-triazol-4-amine, trichloromethane, trimethylamine, 2,2,3-trimethylhexane, 2,2,6-trimethyloctane
Chronic liver disease	Acetaldehyde, acetone, acetophenone, ammonia, 2-butanone, caryophyllene, decene, dimethyl selenide, dimethyl sulphide, ethanol, heptene, indole, isoprene, isopropanol, limonene, methanol, 3-methylbutanonitrile, 2-methylhexane, 3-methylhexane, 2-methylpropene, 1-(methylthio)propane, nonane, (*E*)-2-nonene, octane, octene, pentane, 2-pentanone, 3-pentanone, 2-pentylfuran, phenol, α-pinene, β-pinene, propanol, styrene, α-terpinene, γ-terpinene, tetradecane, tridecane, trimethylamine
Diabetes	Acetone, dimethyl sulphide, ethanol, isoprene, isopropanol, methanol
Malaria	Acetone, allylmethylsulphide, benzene, 3-carene, cyclohexanone, 2,2-dimethyldecane, 3,6-dimethyldecane, 3,7-dimethyldecane, ethylbenzene, ethylcyclohexane, 2-ethylhexanol, hexanal, 4-hydroxy-4-methylpentan-2-one, isoprene, 1-(methylthio)propane, methylthiopropene, methylundecane, nonanal, α-pinene, propylcyclohexane, toluene, tridecane, 2,2,3-trimethylhexane, 2,3,5-trimethylhexane

systems, facilitates data storage and cloud-based analysis, providing a seamless interface for remote monitoring. These advancements pave the way for non-invasive, portable diagnostic tools that could greatly enhance chronic disease management and early detection. Type 2 diabetes mellitus (T2DM) is a prevalent chronic metabolic disease that requires continuous monitoring of blood glucose levels. Currently, diabetes diagnosis methods are invasive and may cause discomfort to patients, such as fingertip blood sampling tests. Kapur *et al.*[155] designed a portable, non-invasive diabetes detection device called 'DiabeticSense'. The device used cutting-edge MOS electrochemical sensors to detect acetone levels in the patient's breath. Since commercial MOS sensors perform non-specific detection of acetone, the researchers trained a ML model to diagnose diabetes. The device also uses IoT technology for cloud-based management of test data and a user-friendly human-machine interface. Widanaarachchige *et al.*[156] reported the development of a ferrocene-encapsulated zeolitic imidazolate framework integrated into a ZeNose platform for the simultaneous detection of four breath biomarkers—ethanol, isopropanol, acetic acid, and acetone. Utilizing chronoamperometry as the transduction principle, the system demonstrated high sensitivity, linear response characteristics, and reliable detection capabilities across the tested VOCs. Importantly, the authors validated the sensor's accuracy through spike-and-recovery experiments, achieving recovery rates within the CLSI guideline range of 80–120%. Such results highlight not only the feasibility of detecting multiple low-concentration biomarkers in exhaled breath but also the potential of metal–organic framework-based architectures to improve stability and reproducibility. This work exemplifies the transition from single-gas to multi-marker platforms, aligning with the trend of using VOC-patterns rather than individual compounds for disease detection.

While pattern-recognition strategies have significantly improved the specificity of VOC-based diagnostics, their successful translation into clinical practice also depends on overcoming the challenge of low analyte concentrations. Exhaled biomarkers such as aldehydes, ketones, or NO are often present in sub-ppm to ppb levels, requiring either pre-concentration steps or the development of highly sensitive sensing architectures. Strategies such as adsorption-based enrichment, solid-phase microextraction, and cryogenic trapping have been employed to increase VOCs availability, while advanced electrode materials with hierarchical nanostructures, catalytic additives, and heterojunction engineering have been designed to directly detect VOCs at ultra-low concentrations. These approaches represent complementary routes to overcoming the low-concentration barrier and advancing VOC-based breath diagnostics toward clinical translation.

In the overall framework of breath analysis technology, although traditional gas sensors mainly focus on the detection of VOCs, this only reveals part of the chemical information in the breath. EBC, collected from condensed water vapor produced during human respiration, capturing a range of biomarkers from within the body. This non-invasive sample offers a fresh perspective on disease detection and epidemiological research, particularly in the context of inflammatory diseases.[157,158] EBC contains numerous inflammatory markers, including cytokines, enzymes, and oxidative stress products, all of which are closely associated with the onset and progression of respiratory diseases. This capability is especially valuable in monitoring chronic respiratory diseases, infectious diseases, and respiratory inflammation,[159–161] including conditions such as asthma,[162,163] COVID-19,[164,165] and COPD.[166,167] Especially in the application of smart mask technology, the combination of EBC detection and traditional gas sensors can not only achieve real-time and portable VOCs monitoring, but also provide a more comprehensive physiological status assessment and disease risk warning through the detection of liquid phase components. Therefore, discussing the application of EBC detection in smart masks not only enriches the diversity of breath analysis technology, but also provides a new idea for the future development of cross-mode sensors.

Smart masks, as a new type of wearable device, have attracted considerable attention. These masks typically use the condensation principle to efficiently collect EBC.[162,164,168] The mask is internally designed with efficient airflow channels to capture water vapor from exhaled air *via* a condensation mechanism. When the user exhales, the water vapor in the breath condenses into liquid upon contact with the cooled surface, facilitating the collection of EBC. This condensation process effectively concentrates the biomarkers in the breath, making subsequent analysis more sensitive and accurate. Cao *et al.* proposed a real-time, continuous wearable mask for monitoring H_2O_2 in exhaled breath condensate.[162] The condensation device was designed using computational fluid dynamics, incorporating microchannels with a secondary flow structure to reduce the size of the exhaled breath condensate device and improve condensation efficiency. The condensation chip, miniaturized three-electrode detection circuit, and real-time display were integrated into the N95 mask for wearable detection. This wearable sensor can be extended to the detection of ions, glucose, nucleic acids, and other substances in exhaled breath condensate (Fig. 8a). Integrating biosensing technology, Daniels *et al.*[164] offered a convenient and efficient COVID-19 rapid screening solution. The mask-based EBC collection system uses a commercial face mask fitted with an engineered EBC collector system based on a Teflon-coated cooling trap. Real-time detection of COVID-19 biomarkers in breath is achieved through an embedded biosensor. These sensors are based on immune response principles, with electrodes pre-modified with a specific aptamer, a nucleic acid sequence with high affinity for the SARS-CoV-2 virus S1 protein. When the aptamer on the electrode binds to the virus, it causes a change in current, which can be measured by the electrochemical biosensor

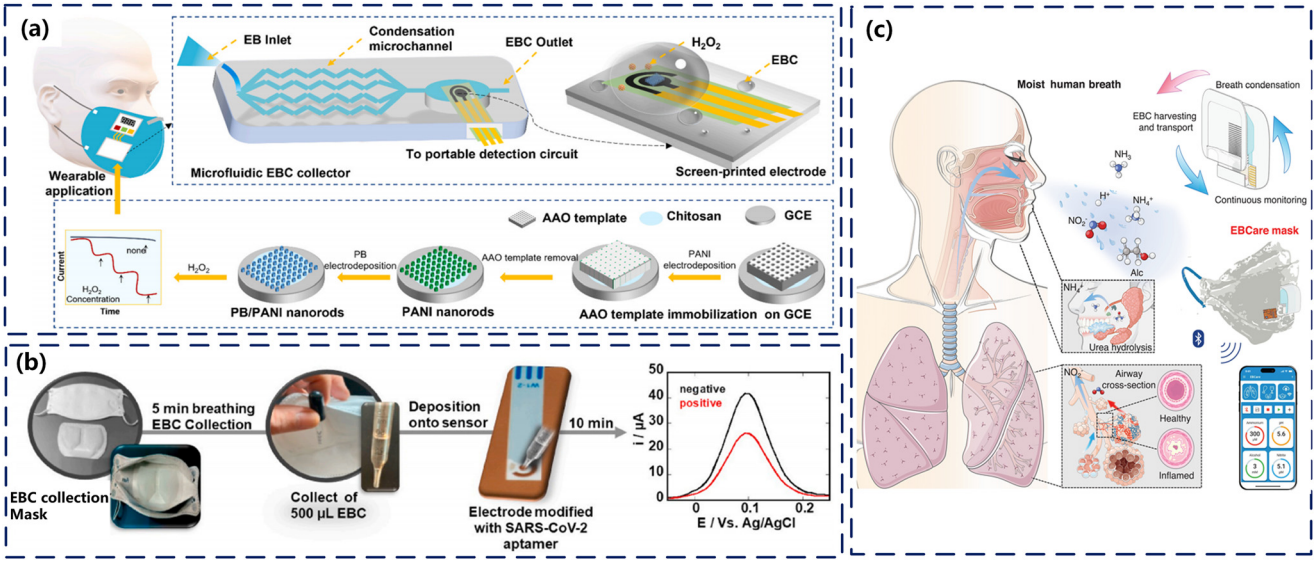

Fig. 8 (a) Illustration of wearable condensation mask for electrochemical monitoring of H_2O_2 in EBC. Reprinted with permission from ref. 162. Copyright 2023 Elsevier. (b) EBC-based diagnostic strategy for SARS-CoV-2 infectivity. Reprinted with permission from ref. 164. Copyright 2021 Elsevier. (c) A smart EBCare mask for efficient harvesting and continuous analysis of exhaled breath condensate. Reprinted with permission from ref. 168. Copyright 2024 AAAS.

(Fig. 8b). Heng *et al.* designed the 'EBCare' smart mask based on a cooling strategy, automated microfluidics, highly selective electrochemical biosensors, and wireless reading circuits.[168] EBCare integrates multiple electrochemical sensors for real-time analysis of key biomarkers in EBC, such as NO_2^-, alcohol, NH_4^+, pH, and temperature sensors. EBCare transmits the collected data in real-time *via* a wireless module to smart devices or the cloud, allowing users to view analysis results instantly, assisting in health management or disease monitoring (Fig. 8c).

The development of smart mask platforms such as EBCare illustrates the potential of integrating electrochemical sensing with wearable technologies for continuous and non-invasive health monitoring. While such systems demonstrate the feasibility of real-time breath analysis, they also highlight the need to evaluate electrochemical gas sensors in disease detection relative to conventional biosensing approaches.

Electrochemical gas sensors analyze VOCs and inorganic gases in exhaled breath, providing non-invasive insights into metabolic and pathological states. For instance, acetone levels in exhaled breath have been reported as potential biomarkers for diabetes, reflecting altered fat metabolism,[169] while aldehydes such as hexanal are linked to lipid peroxidation in lung cancer, and NO serves as a well-recognized marker for asthma. However, these analytes are typically present at ppb–ppt levels, making their detection highly dependent on advanced electrode materials and signal-processing strategies. In contrast, conventional electrochemical biosensors are designed to detect biomarkers in blood, saliva, or urine, such as glucose, lactate, cholesterol, DNA, or proteins, usually present at μM–mM concentrations. A classic example is the electrochemical glucose biosensor (blood glucose meter), which employs glucose oxidase as a recognition element to achieve rapid and specific quantification, revolutionizing diabetes management.[170] Similarly, lactate biosensors are widely used in sports medicine and critical care to monitor tissue hypoxia.[171] These biosensors exhibit high specificity through the use of enzymes, antibodies, or nucleic acid probes, and have already achieved extensive clinical translation. To bridge the gap between these two paradigms, bioinspired platforms such as the electronic nose and electronic tongue have been developed.[172] The electronic nose employs sensor arrays to mimic olfactory detection of complex gas mixtures, while the electronic tongue replicates gustatory sensing to analyze liquid-phase biomarkers. Together, these technologies enable cross-modal sensing of both gaseous and liquid analytes, offering a more holistic assessment of physiological states.

Comparison between the two sensor types highlights both complementarity and divergence. Gas sensors offer portability, real-time detection, and the unique advantage of non-invasive breath sampling, but they face challenges in selectivity, low analyte concentrations, and baseline drift. Biosensors, on the other hand, are more established and benefit from well-validated recognition elements, yet they require invasive sample collection and may not be suitable for continuous monitoring. The integration of these two paradigms—combining breath VOC analysis with biochemical sensing of body fluids—could provide a more comprehensive diagnostic framework, enabling both rapid screening and precise confirmation of disease states.

4.3 Microfluidic integration

Microfluidics has increasingly been recognized as a transformative platform for gas sensing because it offers

precise fluid manipulation, scalable fabrication, and seamless integration with electrochemical and other transduction systems. Yeganegi *et al.*[173] provided a comprehensive review of microfluidic-based gas sensors, outlining how the field has progressed from simple flow-guiding devices to multifunctional analytical platforms capable of sampling, conditioning, and detecting trace analytes. Their analysis emphasized that microchannels provide not only a miniaturized conduit for gas transport but also a controllable microenvironment where factors such as residence time, diffusion length, and adsorption dynamics can be systematically engineered to improve sensitivity and selectivity. Importantly, they highlighted the translation of these devices from environmental and industrial monitoring toward biomedical and healthcare applications, reflecting a broader trend in lab-on-chip research. In parallel, Ramya *et al.*[174] examined the synergy between microfluidics and advanced nanomaterial synthesis for gas sensing. They reported that both continuous-flow and droplet-based microfluidic strategies are increasingly used to fabricate nanostructured sensing elements with improved reproducibility, surface area, and catalytic activity. Such microfluidic-assisted material synthesis not only supports high-performance sensing at the device level but also reduces variability compared to bulk preparation methods. Furthermore, they emphasized that microfluidics provides an inherently scalable route to integrate novel sensing materials —such as MOFs, 2D materials, and hybrid composites—into compact sensor architectures. By combining material innovation with the geometric and fluidic control of microchannels, Ramya *et al.* positioned microfluidic gas sensors as a promising bridge between nanoscale design and system-level healthcare applications. Both approaches converge on the vision of portable, integrated platforms capable of addressing the unique challenges of breath analysis and disease monitoring, thereby establishing a foundation for the next generation of electrochemical gas sensors.

Recent work has increasingly emphasized how microchannel design and electrode architecture directly influence the performance of integrated electrochemical gas sensors. Kaaliveetil *et al.*[34] demonstrated that the use of ionic liquid electrolytes combined with non-planar microelectrodes in microfluidic channels provides an efficient route toward miniaturized gas sensors with improved stability and selectivity. Their study highlighted how the geometry of the electrodes within the microchannel affects diffusion pathways, charge transport, and overall sensitivity, thereby underscoring the interplay between microfluidic structure and electrochemical transduction. The adoption of ionic liquids was particularly important for enabling wide electrochemical windows and enhanced gas solubility, features that are crucial for detecting trace analytes under variable environmental conditions. Bonnema *et al.*[175] investigated how the surface properties of microchannels, including metal coatings and applied surface charges, can be used to tune analyte selectivity in microfluidic-based gas analyzers. By systematically varying the channel coatings (Au, Cu, Ag) and introducing controlled electric fields, they showed that the transient response patterns of alcohols and ketones could be deliberately altered. This revealed that even without changing the sensing element itself, microchannel surface engineering could introduce a new dimension of selectivity through controlled adsorption and desorption processes. Their findings confirm that microchannels should be viewed not merely as passive conduits but as active selectivity elements, capable of shaping the analyte-specific time-domain signatures that reach the detector.

Microfluidic platforms have also begun to establish themselves as enabling technologies for healthcare, where controlled fluid handling and integration with sensing units are critical for reliable biomarker detection. Abouali *et al.*[176] presented a continuous, high-throughput plasma separation device designed to support downstream biosensing. Their system employed hydrodynamic effects within a carefully engineered microchannel to achieve label-free separation of plasma from whole blood, thus providing a stable and clog-resistant source of biofluid for subsequent electrochemical assays. This approach underscores how microchannels can act not only as sample preparation modules but also as reliability-enhancing components in integrated biosensing systems.

Wearable sensing represents another frontier where microfluidics has demonstrated clear advantages. Jiang *et al.*[177] reported a skin-interfaced, flexible microfluidic device capable of long-term and reliable monitoring of uric acid and pH in sweat. By embedding microchannels into a soft substrate that conforms to skin, the device ensured consistent sweat collection and guided analyte flow toward embedded electrochemical sensors. The authors showed that this architecture minimized evaporation losses and mechanical instabilities, which are common problems in wearable biochemical sensing. Their findings illustrate how microchannels can bridge human physiology with sensor electronics, creating stable platforms for personalized healthcare. Menon *et al.*[178] developed a fully automated microfluidic–electrochemical biosensing platform that integrates fluidic control, impedance spectroscopy, and real-time pressure sensing, achieving high sensitivity and sequence specificity for nucleic acid detection. Together, these studies highlight how microfluidic–electrochemical integration enables robust, automated, and versatile biosensing solutions with direct relevance to healthcare diagnostics. In another contribution, Kaaliveetil *et al.*[179] emphasized that microfluidic integration enhances not only the precision of liquid-phase assays but also supports multi-analyte detection, a capability increasingly demanded in both clinical and environmental surveillance. Li *et al.*[180] developed a high-frequency ultrasound-assisted microfluidic chip that integrates surface acoustic waves (SAWs) with a three-electrode electrochemical sensor for rapid biosensing. The acoustic streaming generated near the electrode enhanced

mass transport, improving diffusion by 41%, while boosting sensitivity up to 17-fold for glucose detection. This work demonstrates the potential of SAW-driven microfluidics to achieve highly sensitive, fast, and biocompatible point-of-care electrochemical diagnostics. These studies collectively demonstrate that the value of microfluidic integration extends well beyond sample delivery: it provides robustness, multiplexing capacity, and adaptability across diverse biosensing contexts. These capabilities pave the way for their more extensive integration with electrochemical gas sensors, particularly in breath analysis and organ-on-chip studies where gases serve as key indicators of health and disease.

In conclusion, we believe that opportunities exist in several directions. First, cross-modal integration of microfluidic gas sensors with liquid-phase biosensors—akin to the "electronic nose" and "electronic tongue" concepts—could enable holistic physiological monitoring through simultaneous analysis of VOCs, electrolytes, and metabolites. Second, the incorporation of machine learning into transient microfluidic fingerprints offers a route toward robust analyte recognition and adaptive drift correction in real time. Third, advances in flexible substrates and wearable designs, as demonstrated by Jiang *et al.*,[177] suggest that microfluidics can be embedded directly into skin-mounted or mask-based health monitors. Finally, clinical translation will require standardized fabrication and validation protocols, ensuring reproducibility across populations and deployment conditions. Collectively, these developments set the stage for deeper integration of microfluidics with electrochemical gas sensors. By combining structural engineering, material innovation, and healthcare-focused design, microchannels can transform traditional sensors into multifunctional diagnostic platforms. This provides a natural transition to the next section of this review, where the coupling of electrochemical gas sensing principles with microfluidic architectures is explored in detail to address the challenges of disease detection through volatile biomarkers.

5. Challenges, limitations and perspective

Nowadays, smart electrochemical gas sensor has made remarkable progress with the support of technologies such as the IoT, ML, and self-powered. Through the integration of these advanced technologies, traditional gas sensor equipment is gradually transforming from large, heavy, rigid devices into small, portable, and efficient smart sensor systems. These advances provide more flexible and reliable solutions for human health management. Although smart gas sensors are expected to play a significant role in more complex and diverse scenarios in the future, they still face considerable challenges, as they remain in the early stages of development. This section discusses the challenges and future prospects of smart gas sensors based on electrochemical principles.

Electrochemical gas sensors are known for their high sensitivity and selectivity in gas detection, but they still face significant constraints in terms of cross-interference, limited operational lifespan, response times and sensitivity to environmental conditions. The selectivity of electrochemical gas sensor is mainly determined by the characteristics of electrode material and electrolyte. Due to the large differences in the characteristics of gas molecules, gas sensors are usually able to selectively identify different gases, but they are also susceptible to cross interference from other gases. In real-world conditions, exhaled breath and ambient air contain complex mixtures of interfering gases with overlapping redox potentials, making it difficult for sensors to discriminate target biomarkers. Although advances in catalytic modification, molecular sieving membranes, and nanostructured materials have partially improved selectivity, further innovations in material design and hybrid systems are still required. Another important challenge is the response and recovery dynamics of electrochemical gas sensors. While high sensitivity is crucial, many sensing materials suffer from slow recovery after gas exposure due to strong adsorption or sluggish desorption kinetics, leading to incomplete baseline return. This limitation restricts their use in real-time monitoring scenarios such as breath analysis and air quality surveillance. In parallel, selectivity remains a long-standing challenge, as interfering gases with similar redox potentials and environmental factors such as humidity can significantly affect sensor accuracy. Addressing these issues requires rational material design (*e.g.*, surface functionalization,[181] hierarchical nanostructures[182]) to accelerate gas desorption and enhance molecular recognition. Besides, the working principle of electrochemical sensors relies on the reaction between electrodes and electrolytes, both of which are prone to corrosion. Over time, the electrode material may corrode or degrade, resulting in unstable sensor output or reduced accuracy, ultimately affecting the reliability and service life of the sensor. Because these reactions take time to complete, electrochemical sensors tend to have relatively long response times, especially when detecting low concentrations of gases, which makes rapid, real-time monitoring difficult to achieve. Furthermore, the performance of electrochemical gas sensors is significantly affected by environmental factors. Temperature fluctuations will change the reaction rate of the electrode surface, and humidity will affect the conductivity of the electrolyte, resulting in a deviation of the sensor output signal.[183] Therefore, compensation and calibration methods, such as the calibration formula,[135] are necessary to ensure accurate measurements under different environmental conditions. Algorithms such as baseline subtraction,[184] adaptive filtering, and drift-compensating neural networks[185] show promise for enabling continuous monitoring without frequent recalibration.

IoT technology is the backbone of intelligent system development and application, but common issues persist. IoT systems require real-time data collection, storage, and

analysis, placing higher demands on the processing power, storage capacity, and computational resources of electrochemical gas sensors. Over-reliance on cloud computing solutions can cause delays in certain scenarios, affecting real-time sensor responsiveness. Additionally, the hardware aspect of IoT systems should focus on miniaturization and low power consumption to meet the demands of portable and wearable devices (such as smart masks[164,168] and smart shirts[137]). While IoT technology allows for remote monitoring of gas sensors, network connections may be unstable in some remote areas or harsh environmental conditions, which can affect data transmission and real-time feedback. In large-scale deployments, ensuring stable communication between sensors and the cloud platform remains a challenge. Furthermore, with the widespread use of IoT devices, data security and privacy protection have become urgent issues. Given that gas sensors involve sensitive data such as health tracking, ensuring that this data is not tampered with or leaked is a key challenge for IoT systems.

One of the core challenges in self-powered technology is efficiently storing and managing the generated electrical energy. While TENGs and PENGs can collect energy from the environment, the key to large-scale application lies in how to stabilize and manage this energy using efficient energy storage devices (such as supercapacitors,[186,187] rechargeable batteries,[188,189] *etc.*), due to their unstable or intermittent output. Furthermore, the performance of TENGs and PENGs is closely related to environmental conditions. External factors such as temperature, humidity, and air pollution can negatively affect the performance of friction or piezoelectric materials, reducing energy transduction efficiency. In extreme environments, ensuring the stability and reliability of these self-powered systems remains a critical issue. Research should focus on improving energy efficiency and reducing energy consumption by optimizing sensor design. In summary, while TENGs and PENGs show potential as self-powered technologies, they face numerous technical challenges. Future research must address these limitations by optimizing material selection, designing more efficient energy management systems, and exploring new energy harvesting methods to facilitate the widespread use of TENGs and PENGs in practical applications.

ML is a rapidly evolving technology, but it still faces limitations and challenges in real-world applications. On the one hand, although ML performs well in different gas monitoring tasks, ensuring that the sensor remains well-adapted in dynamic environments is still a problem, on the other hand, ML models can appear overfitting, resulting in poor performance in new environments, affecting the reliability and accuracy of the sensor. Moreover, the output data of electrochemical gas sensors are often affected by environmental factors[190] (such as temperature and humidity changes), and if the data are insufficient or unrepresentative of the target scenario, the model's accuracy and generalization ability will deteriorate. For gas sensitivity of rare gases or complex ambient gases, there are often problems of data collection difficulties and data bias. Additionally, deep learning training typically requires extended computation times and high-performance hardware (such as GPUs,[191] TPUs, *etc.*). This makes deploying deep learning models difficult in certain edge devices or resource-constrained environments, limiting their application in small devices like embedded gas sensors. Future research will need to achieve breakthroughs in improving data processing capabilities, computational efficiency, and solving overfitting issues.

6. Challenges, limitations and perspective

In this review, we first summarize the principles and technical methods of electrochemical sensing, and also present three different operating modes of electrochemical gas sensors with related fabrication techniques. Next, we introduce the developments in IoT, self-powered technologies and ML in recent years, as well as the changes and development trends they bring to smart electrochemical gas sensors. Then, we proceed to introduce the applications in three fields: air monitoring, breath detection and microfluidic integration. Finally, we discuss and summarize the limitations of the development of smart electrochemical gas sensors, and provide an outlook on their future development.

We are fully confident that smart electrochemical gas sensors will bring revolutionary progress not only in healthcare but also in environmental monitoring, public safety, and industrial control. The limitations of current technologies, such as sensitivity, selectivity, stability, and self-powered capabilities, will be addressed through innovations in new materials, micro-nano fabrication, intelligent signal processing, and integrated energy management. Notably, the combination of the IoT and ML enables electrochemical gas sensors to deliver more efficient and accurate real-time analysis, providing strong support for personalized healthcare. Additionally, future sensing systems will expand their application areas, merging with multimodal sensing technologies to create adaptive and predictive smart monitoring networks, thereby offering greater value in fields such as smart healthcare, smart cities, and sustainable development.

Author contributions

Hongyang Guo: writing – original draft, review & editing, visualization. Zhuoru Huang: writing – original draft, investigation. Xiaojing Zhang: writing – review & editing. Haoting Zhang: investigation. Jiaying Sun: writing – original draft. Yuzi Zeng: writing – original draft. Yanjie Hu: investigation. Yong Zhou: investigation. Hao Wan: writing –

review & editing. Ping Wang: supervision, project administration.

Conflicts of interest

The authors declare that they have no known competing financial interests or personal relationships that could have appeared to influence the work reported in this paper.

Data availability

No primary research results, software or code have been included and no new data were generated or analysed as part of this review.

Acknowledgements

This work was supported by the National Natural Science Foundation of China (Grant No. 62120106004), National Key Research and Development Program of China (Grant No. 2022YFC2401901), Natural Science Foundation of Zhejiang Province (Grant No. LBY21H180001).

References

1 A. Sharma, R. Kumar and P. Varadwaj, *Mol. Diagn. Ther.*, 2023, **27**, 321–347.
2 M. Kaloumenou, E. Skotadis, N. Lagopati, E. Efstathopoulos and D. Tsoukalas, *Sensors*, 2022, **22**, 1238.
3 M. C. Magnano, W. Ahmed, R. Wang, M. B. Marusic, S. J. Fowler and I. R. White, *TrAC, Trends Anal. Chem.*, 2024, **176**, 117739.
4 R. López, M. Aznar, J. Cacho and V. Ferreira, *J. Chromatogr. A*, 2002, **966**, 167–177.
5 Z. Wang, Y. Zhang, X. Huang, H. Wang, J. Zhao, C. Li, M. Zhu and K. Chen, *Sens. Actuators, B*, 2024, **405**, 135370.
6 W. Chen, S. Qiao, Z. Zhao, S. Gao, Y. Wang and Y. Ma, *Microw. Opt. Technol. Lett.*, 2024, **66**, e33780.
7 J. Li, C. Sun, Q. Li, X. Xu, B. Li, Y. Tian, D. Zheng, R. Yao, K. Yuan and Z. Guo, *ChemSusChem*, 2025, **18**, e202401313.
8 Y. Gu, B. Huang and H. Zhu, *IEEE Sens. J.*, 2025, **25**, 2125–2140.
9 L. Mahmood, M. Ghommem and Z. Bahroun, *J. Appl. Comput. Mech.*, 2023, **9**, 775–803.
10 B. Zong, S. Wu, Y. Yang, Q. Li, T. Tao and S. Mao, *Nano-Micro Lett.*, 2025, **17**, 54.
11 B. Lee, J. Lee, J.-O. Lee, Y. Hwang, H.-K. Bahn, I. Park, S. Jheon and D.-S. Lee, *Sens. Actuators, B*, 2024, **409**, 135578.
12 L. Jiang, Q. Li, S. Lv, B. Wang, S. Pan, P. Sun, J. Zheng, F. Liu and G. Lu, *ACS Sens.*, 2024, **9**, 1575–1583.
13 M. Khokhar, *J. Breath Res.*, 2024, **18**, 024001.
14 Y. Colleaux, C. Willaume, B. Mohandes, J.-C. Nebel and F. Rahman, *Sensors*, 2025, **25**, 1423.
15 T. Seesaard, K. Kamjornkittikoon and C. Wongchoosuk, *Sci. Total Environ.*, 2024, **951**, 175696.
16 A. R. Winter, Y. Zhu, N. G. Asimow, M. Y. Patel and R. C. Cohen, *ACS Sens.*, 2025, **10**, 4329–4335.
17 X. Xu, W. Meng, F. Kong, B. Yan, S. Zheng, X. Li, J. Zhu, Z. He, Y. Li, W. Meng, L. Dai and L. Wang, *Chem. Eng. J.*, 2025, **507**, 160603.
18 X. Sun, K. Zhou, H. Ma, X. Zhang, X. Zhong and W. Lu, *J. Cleaner Prod.*, 2025, **495**, 145052.
19 Q. Liu, F. Zhang, M. Pei and W. Jiang, *Micromachines*, 2024, **15**, 737.
20 A. Kumaravel and S. Sathyamoorthi, *Environ. Eng. Sci.*, 2024, **41**, 79–94.
21 S. Luo, M. Su, X. Yang, Z. Ning, H. Liu, S. Wang and L. Wang, *J. Chem. Technol. Biotechnol.*, 2024, **99**, 872–879.
22 A. Parihar, P. Sharma, N. K. Choudhary, R. Khan and E. Mostafavi, *Environ. Pollut.*, 2024, **351**, 124029.
23 J. Zhang, Z. Li, H. Yang, W. Chen, Z. Wang, H. Zhou, P. Li and X. Sun, *Food Chem.*, 2024, **460**, 140620.
24 M. Nami, M. Taheri, I. A. Deen, M. Packirisamy and M. J. Deen, *TrAC, Trends Anal. Chem.*, 2024, **174**, 117664.
25 C. Hao, *Molecules*, 2024, **29**, 1106.
26 L. Chen, J. Geng, Z. Guo and X.-J. Huang, *TrAC, Trends Anal. Chem.*, 2023, **167**, 117233.
27 W. Zhang, X. Chen, Y. Xing, J. Chen, L. Guo, Q. Huang, H. Li and H. Liu, *Molecules*, 2024, **29**, 5.
28 S. Atkare, C. S. Rout and S. Jagtap, *Mater. Adv.*, 2024, **5**, 1440–1453.
29 X. Cao, Y. Xiong, J. Sun, X. Xie, Q. Sun and Z. L. Wang, *Nano-Micro Lett.*, 2023, **15**, 14.
30 I. Banga, A. Paul, D. C. Poudyal, S. Muthukumar and S. Prasad, *ACS Sens.*, 2023, **8**, 3307–3319.
31 Z. Zhang, P. Qiu, Y. Deng and W. Luo, *Small Methods*, 2025, **9**, e2500228.
32 Y. H. Liu, Y. Qi, Y. J. Cai, X. Y. Bao and S. Gao, *Photoacoustics*, 2025, **43**, 100715.
33 A. Agarwal, L. Torrent, J. Indlekofer, H. Madi, L. P. Culleton, S. M. A. Biollaz and C. Ludwig, *Bioresour. Technol.*, 2025, **429**, 100715.
34 S. Kaaliveetil, Y.-Y. Lee, Z. Li, Y.-H. Cheng, N. H. Menon, S. Dongare, B. Gurkan and S. Basuray, *J. Electrochem. Soc.*, 2023, **170**, 087508.
35 M. Singh and K. Won, *Microchem. J.*, 2025, **208**, 112444.
36 Z. Deng, Y. Liu and Z. Dai, *Chem. – Asian J.*, 2023, **18**, e202201160.
37 J.-H. Lee, J.-H. Shin, K.-D. Seo, D.-S. Park and Y.-B. Shim, *Sens. Actuators, B*, 2025, **422**, 136657.
38 M. Zhang, L. Yao, Y. Xing, J. Cheng, T. Yang, J. Liu and W. Pan, *J. Mater. Sci. Technol.*, 2024, **181**, 189–197.
39 Y. Zhang, T. Gu, F. Liu, L. Jiang, S. Lv, J. Wang, S. Pan, X. Jia, P. Sun, Y. Gao and G. Lu, *Sens. Actuators, B*, 2023, **390**, 133943.
40 Y. C. Dong, X. Pan, J. F. Xia, M. T. Dai, Z. H. Xue, S. S. Liu, X. T. Dong, J. X. Wang, D. Y. Jiang and Q. Li, *Inorg. Chem. Commun.*, 2024, **170**, 113485.
41 Y. Z. Zhong, N. Lopez-Larrea, M. Alvarez-Tirado, N. Casado, A. Koklu, A. Marks, M. Moser, I. McCulloch, D. Mecerreyes and S. Inal, *Chem. Mater.*, 2024, **36**, 1841–1854.
42 J. Newman and N. P. Balsara, *Electrochemical systems*, 4th edn, Wiley, Hoboken, 2021.

43 N. U. Nazir, S. R. Abbas, H. Nasir and I. Hussain, *J. Electroanal. Chem.*, 2022, **905**, 115977.
44 X. Tian, X. Cui, Y. Xiao, T. Chen, X. Xiao and Y. Wang, *ACS Appl. Mater. Interfaces*, 2023, **15**, 9604–9617.
45 A. Husain and M. U. Shariq, *Sens. Actuators, A*, 2023, **359**, 114504.
46 M. M. Ahmed, R. Zhao, J. Du and J. Li, *J. Electrochem. Soc.*, 2022, **169**, 020573.
47 L. V. Shmygleva, A. V. Chub and L. S. Leonova, *Sens. Actuators, B*, 2021, **349**, 130823.
48 P. S. Kumar, G. Padmalaya, N. Elavarasan and B. S. Sreeja, *Chemosphere*, 2023, **313**, 137345.
49 K. Luo, H. Peng, B. Zhang, L. Chen, P. Zhang, Z. Peng and X. Fu, *Coord. Chem. Rev.*, 2024, **518**, 216049.
50 A. Barhoum, S. Hamimed, H. Slimi, A. Othmani, F. M. Abdel-Haleem and M. Bechelany, *Trends Environ. Anal. Chem.*, 2023, **38**, e00199.
51 H. A. Saputra, *Monatsh. Chem.*, 2023, **154**, 1083–1100.
52 M. Rafiee, D. J. Abrams, L. Cardinale, Z. Goss, A. Romero-Arenas and S. S. Stahl, *Chem. Soc. Rev.*, 2024, **53**, 566–585.
53 H. S. Magar, R. Y. A. Hassan and A. Mulchandani, *Sensors*, 2021, **21**, 6578.
54 Z. Zhi, W. Gao, J. Yang, C. Geng, B. Yang, C. Tian, S. Fan, H. Li, J. Li and Z. Hua, *Sens. Actuators, B*, 2022, **367**, 132137.
55 U. Klun, D. Zorko, L. Stojanov, V. Mirceski and V. Jovanovski, *Sens. Actuators Rep.*, 2023, **5**, 100144.
56 P. Zuo, R. Wang, F. Li, F. Wu, G. Xu and W. Niu, *Talanta*, 2021, **233**, 122539.
57 A. Volkov, E. Gorbova, A. Vylkov, D. Medvedev, A. Demin and P. Tsiakaras, *Sens. Actuators, B*, 2017, **244**, 1004–1015.
58 D. Molino, G. Ferraro, S. Lettieri, P. Zaccagnini, M. Etzi, C. Astorino, E. De Nardo, M. Bartoli, A. Lamberti, C. F. Pirri and S. Bocchini, *Adv. Sustainable Syst.*, 2024, **8**, 2400415.
59 H. Zhang, H. Zhu, H. Su, S. Nie, Y. Zhu, Y. Liu and L. Xu, *Int. J. Hydrogen Energy*, 2024, **54**, 1461–1468.
60 J. Ma, W. Meng, Y. Li, L. Dai and L. Wang, *Sens. Actuators, B*, 2024, **401**, 135058.
61 W. Meng, L. Wang, H. Zhou, Y. Liu and L. Dai, *Sens. Actuators, B*, 2021, **327**, 128874.
62 X. Zhang, J. Sun, K. Tang, H. Wang, T. Chen, K. Jiang, T. Zhou, H. Quan and R. Guo, *Microsyst. Nanoeng.*, 2022, **8**, 67.
63 M. A. Belal, S. Hajra, S. Panda, K. R. Kaja, K. J. Park and H. J. Kim, *Micro Nano Syst. Lett.*, 2025, **13**, 10.
64 M. A. Belal, S. Hajra, S. Panda, K. R. Kaja, K. J. Park, R. Jana, P. Ganga Raju Achary and H. J. Kim, *J. Mater. Sci.: Mater. Electron.*, 2025, **36**, 750.
65 M. A. Belal, S. Hajra, S. Panda, K. R. Kaja, M. M. M. Abdo, A. Abd El-Moneim, D. Janas, Y. K. Mishra and H. J. Kim, *J. Mater. Chem. A*, 2025, **13**, 5447–5497.
66 M. A. Belal, R. Yousry, G. Taulo, A. A. AbdelHamid, A. E. Rashed and A. A. El-Moneim, *ACS Appl. Mater. Interfaces*, 2023, **15**, 53632–53643.
67 A. M. Bayoumy, A. Hessein, M. Ahmed Belal, M. Ezzat, M. A. Ibrahim, A. Osman and A. Abd El-Moneim, *J. Power Sources*, 2024, **617**, 235145.
68 G. T. Taulo, A. E. Moharm, M. A. Belal, N. M. Shaalan, M. M. Ayad, G. G. Mohamed and A. A. El-Moneim, *Sens. Actuators, B*, 2025, **443**, 138186.
69 M. A. Belal, H. H. Khalil, R. L. Mahajan, A. E. Rashed, S. N. Khattab and A. A. El-Moneim, *J. Energy Storage*, 2024, **101**, 113900.
70 Q. Chen and N. Sheng, *Sci. Rep.*, 2024, **14**, 19189.
71 A. Chakraborty, R. Das Gupta, M. Z. Kabir and S. Dhar, *Internet of Things*, 2023, **24**, 100942.
72 C. Cacciuttolo, V. Guzman, P. Catrinir and E. Atencio, *Minerals*, 2024, **14**, 446.
73 K. Lalitha, G. Ramya and M. Shunmugathammal, *IEEE Sens. J.*, 2023, **23**, 21355–21362.
74 Y. Zhuang, X. Wang, P. Lai, J. Li, L. Chen, Y. Lin and F. Wang, *Biosensors*, 2024, **14**, 191.
75 I. Christakis, O. Tsakiridis, D. Kandris and I. Stavrakas, *Electronics*, 2023, **12**, 1842.
76 L. Parri, M. Tani, D. Baldo, S. Parrino, E. Landi, M. Mugnaini and A. Fort, *Sensors*, 2023, **23**, 5060.
77 H. Zhang, R. Ren, X. Gao, H. Wang, W. Jiang, X. Jiang, Z. Li, J. Pan, J. Wang, S. Wang, Y. Ding, Y. Mu, X. Wang, J. Du, W.-T. Li, Z. Xiong and J. Zou, *Water Res.*, 2025, **268**, 122663.
78 D. Hao, L. Qi, A. M. Tairab, A. Ahmed, A. Azam, D. Luo, Y. Pan, Z. Zhang and J. Yan, *Renewable Energy*, 2022, **188**, 678–697.
79 Y. Jia, Q. Jiang, H. Sun, P. Liu, D. Hu, Y. Pei, W. Liu, X. Crispin, S. Fabiano, Y. Ma and Y. Cao, *Adv. Mater.*, 2021, **33**, 2102990.
80 A. Nozariasbmarz, H. Collins, K. Dsouza, M. H. Polash, M. Hosseini, M. Hyland, J. Liu, A. Malhotra, F. M. Ortiz, F. Mohaddes, V. P. Ramesh, Y. Sargolzaeiaval, N. Snouwaert, M. C. Ozturk and D. Vashaee, *Appl. Energy*, 2020, **258**, 114069.
81 L. Liu, X. Guo and C. Lee, *Nano Energy*, 2021, **88**, 106304.
82 A. Nag, R. B. V. B. Simorangkir, S. Sapra, J. L. Buckley, B. O'Flynn, Z. Liu and S. C. Mukhopadhyay, *IEEE Sens. J.*, 2021, **21**, 26415–26425.
83 R. Liu, Z. L. Wang, K. Fukuda and T. Someya, *Nat. Rev. Mater.*, 2022, **7**, 870–886.
84 H. J. Sim, D. Y. Lee, H. Kim, Y.-B. Choi, H.-H. Kim, R. H. Baughman and S. J. Kim, *Nano Lett.*, 2018, **18**, 5272–5278.
85 B. Clerckx, R. Zhang, R. Schober, D. W. K. Ng, D. I. Kim and H. V. Poor, *IEEE J. Sel. Areas Commun.*, 2019, **37**, 4–33.
86 S. Kim, R. Vyas, J. Bito, K. Niotaki, A. Collado, A. Georgiadis and M. M. Tentzeris, *Proc. IEEE*, 2014, **102**, 1649–1666.
87 F.-R. Fan, Z.-Q. Tian and Z. L. Wang, *Nano Energy*, 2012, **1**, 328–334.
88 H. Joo, K. Y. Lee and J.-H. Lee, *Energy Technol.*, 2022, **10**, 2200113.
89 S. Wang, B. Liu, Z. Duan, Q. Zhao, Y. Zhang, G. Xie, Y. Jiang, S. Li and H. Tai, *Sens. Actuators, B*, 2021, **327**, 128923.
90 D. Wang, D. Zhang, Y. Yang, Q. Mi, J. Zhang and L. Yu, *ACS Nano*, 2021, **15**, 2911–2919.

91 Y. Su, S. Chen, B. Liu, H. Lu, X. Luo, C. Chen, W. Li, Y. Long, H. Tai, G. Xie and Y. Jiang, *Mater. Today Phys.*, 2023, **30**, 100951.
92 S. Sardana, H. Kaur, B. Arora, D. K. Aswal and A. Mahajan, *ACS Sens.*, 2022, **7**, 312–321.
93 D. Wang, D. Zhang, J. Guo, Y. Hu, Y. Yang, T. Sun, H. Zhang and X. Liu, *Nano Energy*, 2021, **89**, 106410.
94 D. Wang, D. Zhang, M. Tang, H. Zhang, T. Sun, C. Yang, R. Mao, K. Li and J. Wang, *Nano Energy*, 2022, **100**, 107509.
95 D. Wang, D. Zhang, X. Chen, H. Zhang, M. Tang and J. Wang, *Nano Energy*, 2022, **102**, 107711.
96 B. Liu, Y. Jiang, G. Xie, Z. Duan, Z. Yuan, Y. Zhang, Q. Zhao, Z. Cao, F. Dong and H. Tai, *Chem. Eng. J.*, 2023, **471**, 144795.
97 Y. Su, J. Wang, B. Wang, T. Yang, B. Yang, G. Xie, Y. Zhou, S. Zhang, H. Tai, Z. Cai, G. Chen, Y. Jiang, L.-Q. Chen and J. Chen, *ACS Nano*, 2020, **14**, 6067–6075.
98 C. Cai, J. Mo, Y. Lu, N. Zhang, Z. Wu, S. Wang and S. Nie, *Nano Energy*, 2021, **83**, 105833.
99 D. Zhang, Z. Yang, P. Li, M. Pang and Q. Xue, *Nano Energy*, 2019, **65**, 103974.
100 Y. Niu, J. Zeng, X. Liu, J. Li, Q. Wang, H. Li, N. F. de Rooij, Y. Wang and G. Zhou, *Adv. Sci.*, 2021, **8**, e2100472.
101 S. Fei, M. A. Hassan, Y. Xiao, X. Su, Z. Chen, Q. Cheng, F. Duan, R. Chen and Y. Ma, *Precis. Agric.*, 2023, **24**, 187–212.
102 K. Vos, Z. Peng, C. Jenkins, M. R. Shahriar, P. Borghesani and W. Wang, *Mech. Syst. Signal Process.*, 2022, **169**, 108752.
103 B. Mahbooba, M. Timilsina, R. Sahal and M. Serrano, *Complexity*, 2021, **2021**, 6634811.
104 O. Sagi and L. Rokach, *Inf. Sci.*, 2021, **572**, 522–542.
105 R. Ghosh, S. Phadikar, N. Deb, N. Sinha, P. Das and E. Ghaderpour, *IEEE Sens. J.*, 2023, **23**, 5422–5436.
106 G. Lin, A. Lin and D. Gu, *Inf. Sci.*, 2022, **608**, 517–531.
107 A. A. Movassagh, J. A. Alzubi, M. Gheisari, M. Rahimi, S. Mohan, A. A. Abbasi and N. Nabipour, *J. Ambient Intell. Humaniz. Comput.*, 2021, **14**, 6017–6025.
108 D. Wang, Z. J. Shen, X. Yin, S. Tang, X. Liu, C. Zhang, J. Wang, J. Rodriguez and M. Norambuena, *IEEE Trans. Ind. Electron.*, 2022, **69**, 3689–3699.
109 G.-F. Fan, L. Z. Zhang, M. Yu, W.-C. Hong and S.-Q. Dong, *Int. J. Elec. Power Energy Syst.*, 2022, **139**, 108073.
110 Y.-F. Zhang, Y.-H. Wang, Z.-F. Gu, X.-R. Pan, J. Li, H. Ding, Y. Zhang and K.-J. Deng, *Front. Med.*, 2023, **10**, 1052923.
111 H. Hu, J. Liu, X. Zhang and M. Fang, *Pattern Recognit.*, 2023, **139**, 109404.
112 M. Premkumar, G. Sinha, M. D. Ramasamy, S. Sahu, C. B. Subramanyam, R. Sowmya, L. Abualigah and B. Derebew, *Sci. Rep.*, 2024, **14**, 5434.
113 L. L. Gao, J. Bien and D. Witten, *J. Am. Stat. Assoc.*, 2024, **119**, 332–342.
114 P. An, Z. Wang and C. Zhang, *Inf. Process. Manage.*, 2022, **59**, 102844.
115 Y. An, K. Zhang, Y. Chai, Z. Zhu and Q. Liu, *IEEE Trans. Ind. Inform.*, 2024, **20**, 615–625.
116 F. L. Gewers, G. R. Ferreira, H. F. De Arruda, F. N. Silva, C. H. Comin, D. R. Amancio and L. D. F. Costa, *ACM Comput. Surv.*, 2021, **54**, 70.
117 J. B. Schreiber, *Res. Social Adm. Pharm.*, 2021, **17**, 1004–1011.
118 X. Huang, Y. Li, E. Witherspoon, R. He, G. Petruncio, M. Paige, M. Li, T. Liu, K. Amine, Z. Wang, Q. Li and P. Dong, *ACS Sens.*, 2023, **8**, 3389–3399.
119 M. Chen, M. Zhang, Z. Yang, C. Zhou, D. Cui, H. Haick and N. Tang, *Adv. Funct. Mater.*, 2024, **34**, 2309732.
120 N. S. M. Tombel, H. F. M. Zaki and H. F. B. M. Fadglullah, *IIUM Eng. J.*, 2023, **24**, 407–420.
121 V. Gupta, Z. Mallick, A. Choudhury and D. Mandal, *Langmuir*, 2024, **40**, 8897–8910.
122 Q. Chen, X. Guo, Y. Jiang, X. Liu, S. Xu, X. Huang, Y. Chen, X. Ye, A. Pan, Y. Dong, Z. He and J. Wu, *Adv. Sens. Res.*, 2024, **3**, 2300018.
123 Y. Li, S. Guo, B. Wang, J. Sun, L. Zhao, T. Wang, X. Yan, F. Liu, P. Sun, J. Wang, S. C. Tan and G. Lu, *Infomat*, 2024, **6**, e12544.
124 L. Sun, X. Liu, S. Liu, X. Chen and Z. Li, *Anal. Chem.*, 2023, **95**, 14822–14829.
125 L. Liu, C. Hu, T. Ou, Z. Wang, Y. Zhu and N. Na, *Adv. Intell. Syst.*, 2023, **5**, 2200136.
126 C. Fang, H.-Y. Li, L. Li, H.-Y. Su, J. Tang, X. Bai and H. Liu, *Adv. Intell. Syst.*, 2022, **4**, 2200074.
127 Y. Yu, X. Si, C. Hu and J. Zhang, *Neural Comput.*, 2019, **31**, 1235–1270.
128 Q. Zhai, T. Tang, X. Lu, X. Zhou, C. Li, J. Yi and T. Liu, *Adv. Intell. Syst.*, 2022, **4**, 2200015.
129 S. Y. Heng, K. Z. Yap, W. Y. Lim and N. Ramakrishnan, *Sens. Imaging*, 2024, **25**, 51.
130 Y. M. Lim, A. Leong, K. Z. Yap, V. Swamy and N. Ramakrishnan, *IEEE Sens. J.*, 2024, **24**, 9718–9725.
131 H. Lee, J. Hwang, H. D. Park, J. H. Choi and J.-S. Lee, *IEEE Access*, 2022, **10**, 68138–68150.
132 W. Ku, G. Lee, J.-Y. Lee, D.-H. Kim, J. Lim, D. Cho, S.-C. Ha, B.-G. Jung, H. Hwang, W. Lee, H. Shin, H. S. Jang, J.-O. Lee, J. H. Hwang and K. H. Park, *J. Hazard. Mater.*, 2024, **466**, 133649.
133 S. Ali, T. Glass, B. Parr, J. Potgieter and F. Alam, *IEEE Trans. Instrum. Meas.*, 2021, **70**, 5500511.
134 Z. Idrees and L. Zheng, *J. Ind. Inf. Integr.*, 2020, **17**, 100123.
135 I. Christakis, O. Tsakiridis, E. Sarri, D. Triantis and I. Stavrakas, *Appl. Sci.*, 2024, **14**, 3282.
136 S. Kolozali, L. Chatzidiakou, R. Jones, J. K. Quint, F. Kelly and B. Barratt, *Neural Comput. Appl.*, 2023, **35**, 17247–17265.
137 R. De Fazio, A.-R. Al-Hinnawi, M. De Vittorio and P. Visconti, *Appl. Sci.*, 2022, **12**, 2873.
138 Z. Yang, S. Lv, Y. Zhang, J. Wang, L. Jiang, X. Jia, C. Wang, X. Yan, P. Sun, Y. Duan, F. Liu and G. Lu, *Nano-Micro Lett.*, 2022, **14**, 148.
139 S. Karmakar, M. S. Deepak, O. P. Nanda, A. Sett, P. C. Maity, G. Karmakar, R. Sha, S. Badhulika and T. K. Bhattacharyya, *ACS Appl. Electron. Mater.*, 2024, **6**, 3717–3725.

140 Y. Gorbounov, Z. Dinchev, H. Chen and Ieee, in *2022 30th National Conference with International Participation (TELECOM)*, IEEE, Sofia, Bulgaria, 2022, DOI: 10.1109/TELECOM56127.2022.10017331.
141 D. Meng, D. Liu, G. Wang, Y. Shen, X. San, J. Si and F. Meng, *Appl. Surf. Sci.*, 2019, **463**, 348–356.
142 C. Qu, P. Zhao, C. Wu, Y. Zhuang, J. Liu, W. Li, Z. Liu and J. Liu, *Sens. Actuators, B*, 2021, **338**, 129819.
143 Z. Li, D. Zhang, X. Wang, X. Liu, Y. Yang, C. Du, J. Guo and Y. Zhang, *J. Alloys Compd.*, 2023, **939**, 168777.
144 L. Morawska, P. K. Thai, X. Liu, A. Asumadu-Sakyi, G. Ayoko, A. Bartonova, A. Bedini, F. Chai, B. Christensen, M. Dunbabin, J. Gao, G. S. W. Hagler, R. Jayaratne, P. Kumar, A. K. H. Lau, P. K. K. Louie, M. Mazaheri, Z. Ning, N. Motta, B. Mullins, M. M. Rahman, Z. Ristovski, M. Shafiei, D. Tjondronegoro, D. Westerdahl and R. Williams, *Environ. Int.*, 2018, **116**, 286–299.
145 T. Vinh Van, D. Park and Y.-C. Lee, *Int. J. Environ. Res. Public Health*, 2020, **17**, 2927.
146 E. González, J. Casanova-Chafer, A. Romero, X. Vilanova, J. Mitrovics and E. Llobet, *Sensors*, 2020, **20**, 6225.
147 G. D. Nielsen, S. T. Larsen and P. Wolkoff, *Arch. Toxicol.*, 2017, **91**, 35–61.
148 J. Zhang, F. Lv, Z. Li, G. Jiang, M. Tan, M. Yuan, Q. Zhang, Y. Cao, H. Zheng, L. Zhang, C. Tang, W. Fu, C. Liu, K. Liu, L. Gu, J. Jiang, G. Zhang and S. Guo, *Adv. Mater.*, 2022, **34**, 2109453.
149 C. Liu, Q.-Q. Zou, B. Liu and Y. Zhang, *Rare Met.*, 2024, **43**, 257–266.
150 G. Marques and R. Pitarma, *Electronics*, 2019, **8**, 170.
151 A. K. Pathak, K. Swargiary, N. Kongsawang, P. Jitpratak, N. Ajchareeyasoontorn, J. Udomkittivorakul and C. Viphavakit, *Biosensors*, 2023, **13**, 114.
152 P. C. Moura, M. Raposo and V. Vassilenko, *Clin. Chim. Acta*, 2024, **552**, 117692.
153 P. C. Moura, M. M. Raposo and V. Vassilenko, *Biomed. J.*, 2023, **46**, 100623.
154 N. Vadera and S. Dhanekar, *ACS Sens.*, 2024, **10**, 439–447.
155 R. Kapur, Y. Kumar, S. Sharma, V. Rastogi, S. Sharma, V. Kanwar, T. Sharma, A. Bhavsar and V. Dutt, *J. Clin. Med.*, 2023, **12**, 6439.
156 N. S. M. Widanaarachchige, A. Paul, S. Muthukumar and S. Prasad, *Sens. Diagn.*, 2025, **4**, 723–735.
157 W. Ibrahim, M. J. Wilde, R. L. Cordell, M. Richardson, D. Salman, R. C. Free, B. Zhao, A. Singapuri, B. Hargadon, E. A. Gaillard, T. Suzuki, L. L. Ng, T. Coats, P. Thomas, P. S. Monks, C. E. Brightling, N. J. Greening, S. Siddiqui and E. Consortium, *Sci. Transl. Med.*, 2022, **14**, eabl5849.
158 C. C. Wang, K. A. Prather, J. Sznitman, J. L. Jimenez, S. S. Lakdawala, Z. Tufekci and L. C. Marr, *Science*, 2021, **373**, eabd9149.
159 A. Bhide, M. A. Eldeeb, M. Pali, S. Muthukumar and S. Prasad, *ACS Sens.*, 2023, **8**, 3408–3416.
160 L. D. J. Bos and L. B. Ware, *Lancet*, 2022, **400**, 1145–1156.
161 A. Gholizadeh, K. Black, H. Kipen, R. Laumbach, A. Gow, C. Weisel and M. Javanmard, *RSC Adv.*, 2022, **12**, 35627–35638.
162 Y. Cao, H. Shi, Y. Zheng, Z. Tan, Z. Xie, C. Zhang and Z. Chen, *Sens. Actuators, B*, 2023, **393**, 134189.
163 N. Habib, M. A. Pasha and D. D. Tang, *Cell*, 2022, **11**, 2764.
164 J. Daniels, S. Wadekar, K. DeCubellis, G. W. Jackson, A. S. Chiu, Q. Pagneux, H. Saada, I. Engelmann, J. Ogiez, D. Loze-Warot, R. Boukherroub and S. Szunerits, *Biosens. Bioelectron.*, 2021, **192**, 113486.
165 E. Pretorius, C. Venter, G. J. Laubscher, M. J. Kotze, S. O. Oladejo, L. R. Watson, K. Rajaratnam, B. W. Watson and D. B. Kell, *Cardiovasc. Diabetol.*, 2022, **21**, 148.
166 P. J. Barnes, *J. Allergy Clin. Immunol.*, 2016, **138**, 16–27.
167 S. A. Christenson, B. M. Smith, M. Bafadhel and N. Putcha, *Lancet*, 2022, **399**, 2227–2242.
168 W. Heng, S. Yin, J. Min, C. Wang, H. Han, E. S. Sani, J. Li, Y. Song, H. B. Rossiter and W. Gao, *Science*, 2024, **385**, 954–961.
169 T. Yu, X. Meng, X. Hao, Z. Dong, Y. Wang, S. Sun and P. Cheng, *Sens. Actuators, B*, 2024, **418**, 136273.
170 G. Guan, Q. Liang, Y. Zhao, P. Wang, F. Kong, Y. Zhang, Z. Lin, N. Xing, Z. Xue, Q. Lu and Z. Bin, *Front. Chem.*, 2025, **13**, 1591302.
171 Y. Chen, X. Hu, Q. Liang, X. Wang, H. Zhang, K. Jia, Y. Li, A. Zhang, P. Chen, M. Lin, L. Qiu, H. Peng and S. He, *Adv. Funct. Mater.*, 2024, **34**, 2401270.
172 D. Tibaduiza, M. Anaya, J. Gomez, J. Sarmiento, M. Perez, C. Lara, J. Ruiz, N. Osorio, K. Rodriguez, I. Hernandez and C. Sanchez, *Biosensors*, 2024, **14**, 190.
173 A. Yeganegi, K. Yazdani, N. Tasnim, S. Fardindoost and M. Hoorfar, *Front. Chem.*, 2023, **11**, 1267187.
174 K. Ramya, K. Amreen, I. Pronin, A. Karmanov, N. Yakushova and S. Goel, *Nano Futures*, 2023, **7**, 032004.
175 M. J. S. Bonnema, H. w. Veltkamp, D. Alveringh, R. J. Wiegerink and J. C. Loetters, *J. Micromech. Microeng.*, 2024, **34**, 115002.
176 H. Abouali, F. Keyvani, S. A. Hosseini, S. Srikant and M. Poudineh, *Adv. Healthcare Mater.*, 2025, **14**, 2404193.
177 D. Jiang, X. Liu, W. Zhan, M. Fu, J. Liu, J. He, Y. Li, Y. Li, X. Chen and C. Yu, *Nano Lett.*, 2025, **25**, 1427–1435.
178 N. H. Menon, Y. Beshai and S. Basuray, *IEEE Sens. Lett.*, 2025, **9**, 4501404.
179 S. Kaaliveetil, N. N. Khaja, N. H. Menon and S. Basuray, *Chemosensors*, 2024, **12**, 127.
180 W. Li, L. Han, D. Li and Z. Pu, *Sens. Actuators, B*, 2025, **427**, 137211.
181 C. Park, H. Shin, M. Jeon, S. H. Cho, J. Kim and I. D. Kim, *ACS Nano*, 2024, **18**, 26066–26075.
182 X. Tian, X. X. Cui, Y. W. Xiao, T. Chen, X. C. Xiao and Y. D. Wang, *ACS Appl. Mater. Interfaces*, 2023, **15**, 9604–9617.
183 M. L. Hitchman and J. R. Saffell, *ACS Sens.*, 2021, **6**, 3985–3993.

184 H. Mei, P. Wei, Y. Wang, M. A. Ghadikolaei, N. K. Gali and Z. Ning, *npj Clim. Atmos. Sci.*, 2025, **8**, 296.
185 B. S. Prakasha, P. Xiao, M. J. Esplandiu, J. Q. Yang, D. Navarro-Urrios, J. Rodríguez-Viejo and M. Sledzinska, *ACS Sens.*, 2025, **10**, 2712–2720.
186 L. Kang, S. Liu, Q. Zhang, J. Zou, J. Ai, D. Qiao, W. Zhong, Y. Liu, S. C. Jun, Y. Yamauchi and J. Zhang, *ACS Nano*, 2024, **18**, 2149–2161.
187 Z. Yan, S. Luo, Q. Li, Z.-S. Wu and S. Liu, *Adv. Sci.*, 2024, **11**, 2302172.
188 Z. Tie, Y. Zhang, J. Zhu, S. Bi and Z. Niu, *J. Am. Chem. Soc.*, 2022, **144**, 10301–10308.
189 Z. Wu, H. Wang, Q. Ding, K. Tao, W. Shi, C. Liu, J. Chen and J. Wu, *Adv. Funct. Mater.*, 2023, **33**, 2300046.
190 S. D. Lawaniya, S. Kumar, Y. Yu, H.-G. Rubahn, Y. K. Mishra and K. Awasthi, *Mater. Today Chem.*, 2023, **29**, 101398.
191 X. Zhang, J. Zhou, W. Sun and S. K. Jha, *Comput., Mater. & Continua*, 2022, **72**, 1123–1137.